Spring 5-3-2013

Comparing Vegetation Cover in the Santee Experimental Forest, South Carolina (USA), Before and After Hurricane Hugo: 1989-2011

Giovanni R. Cosentino
Georgia State University

COMPARING VEGETATION COVER IN THE SANTEE EXPERIMENTAL FOREST, SOUTH CAROLINA (USA), BEFORE AND AFTER HURRICANE HUGO: 1989-2011

by

GIOVANNI COSENTINO

Under the Direction of Lawrence Kiage

ABSTRACT

Hurricane Hugo struck the coast of South Carolina on September 21, 1989 as a category 4 hurricane on the Saffir-Simpson Scale. Landsat Thematic mapper was utilized to determine the extent of damage experienced at the Santee Experimental Forest (SEF) (a part of Francis Marion National Forest) in South Carolina. Normalized Difference Vegetation Index (NDVI) and the change detection techniques were used to determine initial forest damage and to monitor the recovery over a 22-year period following Hurricane Hugo. According to the results from the NDVI analysis the SEF made a full recovery after a 10-year period. The remote sensing techniques used were effective in identifying the damage as well as the recovery.

INDEX WORDS: Hurricane damage, Normalized Difference Vegetation Index, Change detection, Hurricane Hugo, Coastal Plain Forest recovery

COMPARING VEGETATION COVER IN THE SANTEE EXPERIMENTAL FOREST, SOUTH CAROLINA (USA), BEFORE AND AFTER HURRICANE HUGO: 1989-2011

by

GIOVANNI COSENTINO

A Thesis Submitted in Partial Fulfillment of the Requirements for the Degree of

Master of Science

in the College of Arts and Sciences

Georgia State University

2013

COMPARING VEGETATION COVER IN THE SANTEE EXPERIMENTAL FOREST, SOUTH CAROLINA (USA), BEFORE AND AFTER HURRICANE HUGO: 1989-2011

by

GIOVANNI COSENTINO

Committee Chair: Lawrence Kiage

Committee: Leslie Edwards

Jeremy Diem

Electronic Version Approved:

Office of Graduate Studies

College of Arts and Sciences

Georgia State University

May 2013

ACKNOWLEDGEMENTS

I would like to thank the faculty members of the Geoscience department at Georgia State University for providing me with the skill set needed to complete my thesis. I would also like to thank my advisor and thesis committee chair, Lawrence Kiage and my committee members, Leslie Edwards and Jeremy Diem for their guidance and support.

TABLE OF CONTENTS

LIST OF TABLES

LIST OF FIGURES

1. INTRODUCTION

Coastal wetland forests are unique environments that contain a wealth of biodiversity. Under ordinary conditions, and without exterior influences, vegetation within a forested area would likely maintain an equilibrium in which species succession is dictated by niche differentiation based on the areas' characteristics (Foster, 1988). However, equilibrium is rarely achieved due to the occurrence of external influences. A disturbance is an interference of an ecosystem by any exterior force that includes hurricanes, floods, and fires, which alter vegetation dynamics and cover (Lugo, 2008). Due to the high concentration of biodiversity within coastal forests and wetlands (Russell et. al., 2002), the initial and sustained impacts caused by natural disasters must be studied. Hurricanes are some of the most significant natural disturbances that affect coastal forest ecosystems in the Southeastern United States (Wang et. al., 2010).

Hurricanes that impact the Southeastern United States are responsible for an extensive amount of damage. In 1989, Hurricane Hugo alone caused an upwards of $1.2 billion in forestry and agricultural damage (Cablk et. al., 1994). A severe hurricane has the capacity to markedly alter the composition of a forested wetland area immediately, initiating long-lasting changes in structure and succession (Foster, 1988; Wang et. al., 2010). This level of destruction merits an investigation of both the initial and sustained impacts caused by this type of natural disaster. Specifically, understanding how certain tree populations react to a hurricane landfall in an area can reveal their susceptibility to reoccurring storms. To develop a more complete understanding of how certain tree populations react to a hurricane landfall in an area, it is essential to study the same area over long time periods, prior to the hurricane and once the hurricane has passed (Frangi & Lugo, 1998). The passage of Hurricane Hugo through the coast of South Caro-

lina in 1989 provided a unique opportunity for a long-term study on how a coastal plain forest responds to a severe natural disaster.

Although many studies (e.g. Cablk et. al., 1994; Hook et. al., 1991; Helm et. al., 1991) have been conducted on the immediate effects of a hurricane on forested areas, little work has focused on the long-term response and recovery of vegetation. This lack of knowledge limits our ability to understand and prevent additional forest destruction caused by events following a severe hurricane (e.g., wild fires and additional habitat loss). It is important to assess the time length for a forested area to begin recovery and to determine whether natural regeneration processes are sufficient to restore the hurricane damaged areas. The current study has two main objectives: 1) to examine the vegetation damage in Francis Marion National Forest due to Hurricane Hugo, specifically in the Santee Experimental Forest subsection; 2) to investigate the regeneration of the vegetation cover over a 20-year period. By reassessing the damage on the native plant species caused by Hurricane Hugo, we can better understand the early phases of revegetation.

1.1 Background Information/Literature Review

Hurricane Hugo developed as a tropical depression off the coast of Africa on September 9, 1989. The storm strengthened as it travelled through the Atlantic before making landfall on the coast of South Carolina on September 21st, 1989, in Charleston, SC (Figure 1) as a Category 4 hurricane with maximum sustained winds of 222 km/h with a barometric pressure of 93.4MPa causing extensive damage to coastal forests (Gresham et. al., 1991; Conner & Inabinette, 2003) A storm of similar magnitude to Hugo is considered to have a return period of 100 years (Cablk et. al., 1994), this emphasizes the importance of understanding the destruction and reestablishment of the coastal plain forests. The eye of Hurricane Hugo came within 8 km of Francis Marion National

Forest (hereafter FMNF) located near Charleston, SC (Hook et. al., 1991Kulkarini, 2004). The FMNF was hit by the upper right quadrant of Hurricane Hugo, which is the area that produces the strongest winds (Foster, 1988). The storm caused a large amount of destruction within the forest and its surrounding areas, making it an important area of interest for studying the aftermath of the hurricane. It was estimated that FMNF sustained a loss of 75% of harvestable timber due to the hurricane (Dunning & Watts, 1991LeGrand, 1990). Figure 1 shows the path of Hurricane Hugo as it encountered the coast of South Carolina.

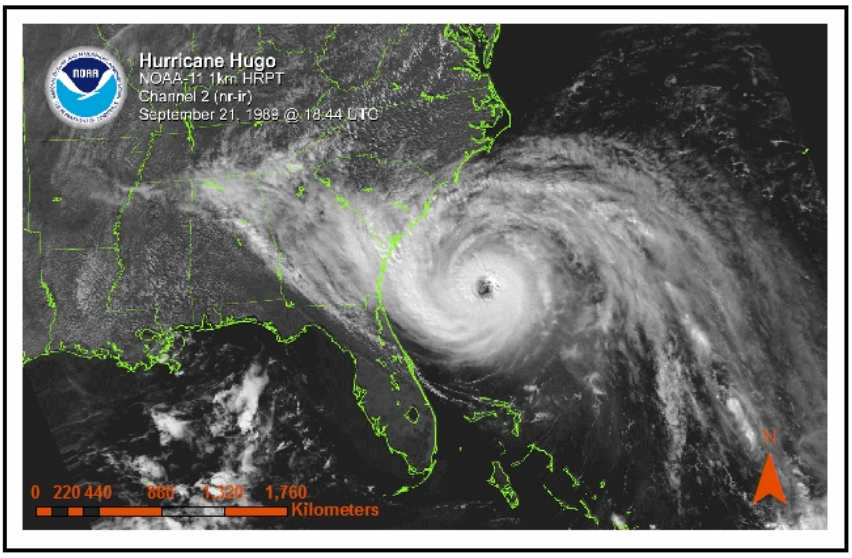

Figure 1 A map of Southeastern United States showing Hurricane Hugo approaching the coast of South Carolina on September 21, 1989.

1.2 Vegetation Damage

There are many factors involved in the type and severity of vegetation damage in an area impacted by a hurricane (Conner & Inabinette, 2003; Gresham et. al., 1991). The key determinants of hurricane vegetation damage on coastal wetland forests include wind speed, age of trees, species involved, and the amount of flooding that oc-

curs. Intense wind speeds can cause severe defoliation and breakage of forested areas (Conner, 1995). Flooding due to storm surge can cause elevated mortality rates for extended periods of time due to the high salinity associated with surge waters (Conner, 1995). Salt water inundation resulting from Hurricane Hugo caused significant damage to six species along the South Carolina coast [i.e., sweetgum (*Liquidambar styraciflua*), red maple (*Acer rubrum*), sugarberry (*Celtis laevigata*), redbay (*Persea borbonia*), waxmyrtle (*Myrica cerifera*), and laurel oak (*Quercus lauriflolia*], (Conner & Inabinette, 2003)].

Along with flood inundation, the age of the tree stand and species present play a key role in the severity of tree mortality. Specifically, the species of tree plays a large role in the variance of tree damage (Gresham et. al., 1991). Species such as live oak (*Quercus virginiana*) and bald cypress (*Taxodium distichum*) have very high resistance to wind damage in the event of a tropical storm, leading to less damage within the species (Gresham et. al. 1991). Longleaf pine (*Pinus palustris*), which is commonly found in the FMNF also exhibited high resistance to wind damage due to the presence of a large taproot and an extensive lateral root system (Gresham et. al., 1991). However, species such as loblolly pine (*Pinus taeda*) and southern red oak (*Quercus falcate*) grow taller making them more susceptible to wind damage in a tropical storm event (Gresham et. al. 1991). Loblolly pine and long leaf pine were the most prevalent tree species in FMNF covering 155,547 acres (65%) prior to Hurricane Hugo in 1989, making the area vulnerable to severe vegetation destruction (Supervisor, 1995).

The severity of forest damage caused by a hurricane is related not only to the species of trees, but the age of trees as well (Foster 1988; Gresham et. al. 1991; Hook et al., 1991). Tree height increases with age, making older trees more susceptible to damage from high wind speeds (Foster, 1988). Susceptibility of conifers to wind damage in-

creases dramatically, after the age of 15 years (Foster, 1988). For instance, in 1938, a hurricane impacted the Harvard Forest, located in Massachusetts and destroyed nearly every conifer species over 30 years old (Foster, 1988). When determining the susceptibility of a forested area to high wind speeds, the age of the tree stands must be considered.

1.3 Detection of Vegetation

Remote Sensing of vegetation change can be classified into four different categories: (1) chlorophyll content, (2) leaf water content, (3) detection based on spectral mixture analysis, and (4) structural changes of damaged forest (Wang et. al., 2010). The first approach utilizes indices such as the NDVI. The NDVI is a well-known and popular method used to detect changes in vegetation over time. NDVI displays the "abundance and activity of chlorophyll absorption of broad-band red wavelengths and chlorophyll reflectance of broad-band near infrared wavelengths" (Myneni et. al., 1995) and can, therefore, display the health of the vegetation in forested areas. NDVI differentiates green vegetation cover from other cover categories due to chlorophyll absorption (Wang et al., 2010). NDVI can be utilized to determine greater information about vegetation rather than using a single channel (Townsend & Walsh, 2001). This is possible because healthy vegetation reflects highly in the near-infrared portion of the electromagnetic spectrum, but very poorly in the red portion (Townsend & Walsh, 2001). NDVI has been effectively used to study forested environments and has been utilized to investigate the damage caused by Hurricane Katrina to forests in the Lower Pearl River Valley (Ramsey, 2001; Rogers et. al., 2009; Wang et. al., 2010). Wang et al. (2010) investigated the accuracy of multiple vegetation detection indices including the enhanced vegetation index (EVI), the normalized difference infrared index (NDII), the leaf area index (LAI) and NDVI. They concluded that NDII, NDVI, and EVI were capable of accurately detect-

ing changes in vegetation cover caused by a hurricane. NDII and NDVI were found to be more sensitive to damage detection and were the indices that provided results similar to the USDA Forest Service analysis (Wang et al., 2010). NDVI is calculated from the ratio between the red band (band 3 in Landsat TM/ETM+, 630-690 nm), which is the chlorophyll absorption region, and the near-infrared (band 4 in Landsat TM/ETM+, 760-900nm) which is scattered by vegetation (Feely et. al., 2005) as follows:

$$NDVI = (NIR-RED)/(NIR+RED), \quad (1)$$

where NIR is the near infrared band, and RED is the red band. Vegetation absorbs energy in the red band wavelength yield little reflectance whereas the satellite sensor detects enhanced reflected from the NIR wavelengths. The NDVI utilizes the contrast in absorption and scattering to estimate vegetation greenness of an area (Feely et. al., 2005). The NDII uses Landsat TM/ETM+ bands 4 and 5 to differentiate between concentrations of plant foliage and seasonal foliage change (Feely et. al., 2005). The NDII is calculated as shown in the following equation:

$$NDVII = (NIR-SWIR)/(NIR+SWIR), \quad (2)$$

where NIR is the near infrared band, and SWIR is shortwave infrared that reflects at 1.24, 1.65 or 2.13 (nm) (Wang, et. al., 2010). NDVI was the band combination chosen in this study rather than NDII because it is more robust and effective and has been proven to be effective in past studies (Cablk et. al., 1994; Ramsey et. al., 2001; Rogers et. al., 2009). This combination of bands was additionally chosen because of the large contrast that exists between the red and the infrared band in these areas of the electromagnetic spectrum.

1.4 Satellite Remote Sensing

Ecosystems are continuously shifting; change in vegetation cover can either be gradual via natural progression or abrupt via natural disturbances or other outside in-

fluences. Hurricanes are capable of causing widespread destruction over large areas in a relatively short period of time. However, the intermittent nature and unpredictable behavior of hurricanes makes it difficult and expensive to monitor their impacts effectively using ground-monitoring techniques. Traditionally, the assessment of a hurricane-impacted forest region has been based on ground surveys, aerial photography, and ecological models, or a combination of these methods (Wang et. al., 2010,). Recently, satellite remote sensing has become the preferred method of monitoring vegetation changes in forested areas caused by hurricanes due to high temporal and spatial resolution, efficiency, predictability, and the relative low cost (Ramsey et. al., 2009). Research on the effectiveness of remote sensing for monitoring post hurricane vegetation change was first conducted in the early 1990s (Wang et. al., 2010). Remote sensing is an important and useful tool because it can be used to generate data when field sampling cannot be used to attain the distribution of vegetation cover (Shuman & Ambrose, 2003). An additional benefit of remote sensing is that it does not disturb the environment during data collection, allowing for the preservation of the actual effects from the natural disaster. This makes remote sensing an ideal tool for detecting damage directly following a natural disaster.

Satellite remote sensing can additionally provide advantages for assessing vegetation inventory and monitoring the growth and recessions of areas with vegetation cover (Ozesmi & Bauer, 2002) Remote sensing images have been used frequently to map and classify vegetation temporal changes (Shuman & Ambrose, 2003). Remotely sensed images have also been used to assess vegetation species composition (Jensen et al., 1985) and to identify plant stress using multispectral reflectance (Anderson & Perry, 1996). Proper selection of satellite imagery has been shown to be just as critical as the choice in sensors in multi temporal change detection (Coppin et. al., 2004). Cer-

tain seasons such as summer and winter (evergreen species) show vegetation to be far more stable than in spring and fall and are therefore the ideal seasons for multi-temporal studies (Coppin et. al., 2004). When selecting multi-temporal satellite images for a study it is important where possible to limit the selection to dates in the same anniversary window. This will minimize the differences in reflectance that is caused by phenology, seasonal differences in vegetation cover, and differences in the sun's angle (Coppin et. al., 2004).

When dealing with land cover change over time, appropriate time intervals between data acquisition dates must be identified. In a previous study investigating re-vegetation in South Carolina, researchers concluded that a two year time period was not a sufficient amount of time in-between two images to detect re-vegetation of an area (Colwell & Thomason, 1998). Three years is the minimum time interval to detect land cover changes from non-forested areas to areas that have begun to reestablish vegetation except where large disturbances are involved (Aldrich, 1975). In order to detect a change from shrubs to the establishment of a forest canopy the suggested interval is 5 to 20 years when utilizing remotely sensed imagery (Park et. al., 1983). Therefore, according to these studies (Coppin et. al., 2004; Colwell et. al., 1980; Aldrich, 1975) change detection intervals should be separated by at least five years in order for re-vegetation detection using satellite imagery. The availability of cloud free images was limited during the 5th and 6th year anniversary window thus, the current study rounded up to 10-year intervals. Additionally, one of the dominant tree species within the SEF longleaf pine spends 5-10 years in a grass stage before making an accent to the canopy. Allowing more time between intervals will ensure that low lying longleaf pine stand will not be mistaken for shrubland/grassland in the unsupervised classification process.

When studying a site affected by a hurricane, it is important to establish the area subjected to the greatest impact. To determine this, the anatomy of a hurricane must be analyzed. The most destructive winds within a hurricane take place on the easterly side (specifically the northeast quadrant), where the combination of rotary velocity and forward movement generate the highest wind speed (Foster, 1988). From this, one would expect the greatest damage to occur in areas that encounter the easterly side of a hurricane. Therefore, in this study, FMNF was chosen as the study site due to its close proximity to the eye of the storm.

1.5 Objectives

The current study investigated temporal times scales needed for a coastal wetland forest to begin to recover from a major disturbance. The overall aim of this study was to investigate the re-vegetation patterns that occur following a major disturbance in a coastal plain forest. Due to the potential effects of hurricane disturbances on the coastal plain forests of South Carolina, FMNF was an ideal study site due to both its location and high levels of natural regeneration. Specifically, the study investigated a subsection of the forest that has experienced little to no human alterations since its establishment in 1937, the Santee Experimental Forest (Hook, et. al., 1991). A land cover change analysis was conducted to determine the primary damage assessment of the effect Hurricane Hugo had on the FMNF in 1989, as well as how the damaged areas recovered after twenty-two years. This study sought to answer the following research questions,

- What was the extent of damage in the Francis Marion National Forest and the Santee Experimental Forest following the landfall of Hurricane Hugo?

- **After a twenty-two year period, to what extent has the Francis Marion National Forest and the Santee Experimental Forest recovered to regain its pre-disturbance vegetation cover?**
- **Can remote sensing be used explicitly to monitor long-term recoveries in coastal plain forest landscapes?**

2. METHODS

2.1 Study Area

The focus of this study was the Santee Experimental Forest, located within the FMNF, which is situated within 8 kilometers of where the eye of Hurricane Hugo made landfall (Hook et. al., 1991). The forest is located on the South Carolina coast, which has been shown to experience hurricane or tropical storm activity once every 2.6 years making this area suitable for post hurricane studies (Cablk et. al., 1994). FMNF contains 258,938 acres and is located within the counties of Charleston and Berkeley in South Carolina (Monitoring and Evaluation Report, 2010). The area extends from approximately 33°27' N to 32°54' N, and 79°59' W to 79°23' W (Figure 2).

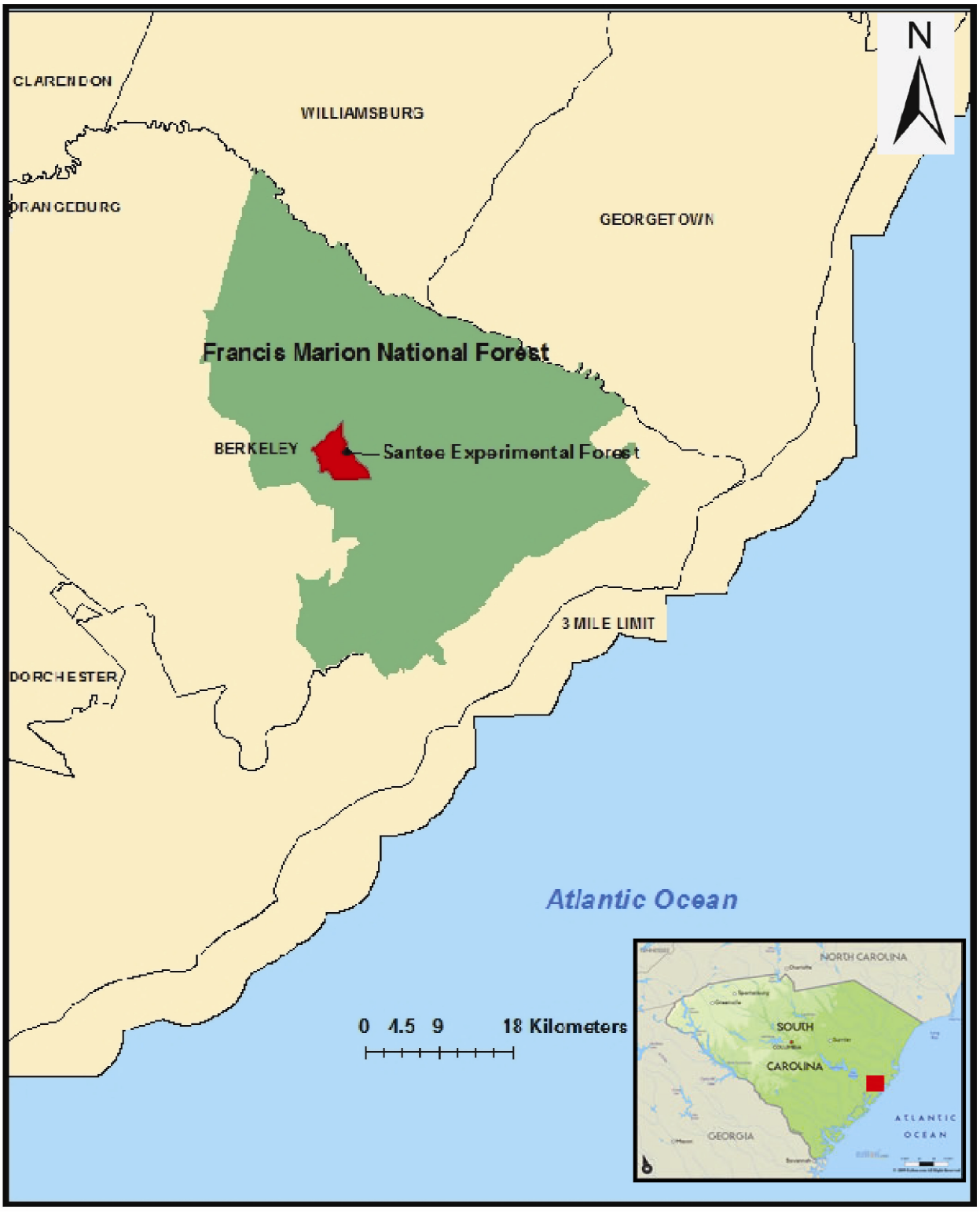

Figure 2 A map showing the location of the Santee Experimental Forest (study area) within Francis Marion National Forest. Inset, the location of the study area marked as a red box on the map of South Carolina.

The Santee Experimental Forest is located approximately 40km from the coast, on the western portion of the FMNF (Hook et. al., 1991). The site spans over 6,100 acres and includes many of the forest types associated with the lower coastal plain regions such as mixed pine hardwood, loblolly pine, longleaf pine, mixed loblolly pine and long-leaf pine, upland hard woods, bottomland hardwoods, and creek swamp containing the tree species shown in Table 1 (Hook et. al., 1991). The age of the stands ranged from 80 to 110 years old (Hook et. al., 1991).

Table 1 Tree species present on the Santee Experimental Forest

Scientific Name	Common Name
Pinus taeda	Loblolly pine
Liqudambar styraciflu	Sweet gum
Quercus falcaya	Southern red oak
Ouercus alba	White oak
Acer rubrum	Red maple
Pinus palustris	Longleaf pine
Quercus vevlutina	Black oak
Quercus pagoda	Cherrybark oak
Quercus michauxii	Swamp chestnut oak
Quercus nigra	Water oak
Fraxinus pennsyl-vania	Green ash
Liriodendron tulipifera	Yellow poplar
Quercus shumardii	Shumard oak
Nyssa sylvatica	Black tupelo
Quercus hemi-sphaerica	Laurel oak
Taxodium disti-chum	Bald cypress
Nyssa aquatica	Water tupelo

This specific area was chosen because, according to U.S Forest Service, it has not been subjected to any logging in the time between Hugo and the present, making it an ideal area for tracking the natural regeneration of vegetation after Hurricane Hugo.

2.2 Data Acquisition

In this study, four satellite remote sensing images were utilized to determine land cover change caused by Hurricane Hugo and the recovery thereafter. The images were acquired by Landsat 5 Thematic Mapper (TM). Landsat 5 was launched on March 1, 1989 and utilizes the thematic mapper (TM) sensor to obtain data. Landsat 7, which was used to acquire the 1999 image was launched on April 15, 1999 and utilizes enhanced thematic mapper (ETM). The combination of the thematic sensor's red and near-infrared band is best suited for determining temporal vegetation change.

In order to accurately assess the land cover change at the Santee Experimental Forest, cloud free satellite images were obtained for four different periods. The image used to represent pre-Hugo vegetation (Figure 3) was acquired on October 30, 1987. The rationale for the selection of the 1987 image was that all images in 1988 that were in the proper time frame had cloud cover over the study area. This image was selected because it represented a time period prior to Hugo and was one of the clearest images near the date of the storm in 1989. The image used to represent post-Hugo vegetation (Figure 4) was acquired on October 03, 1989. This was the only cloud free images within a 30-day period after landfall. The third image used to represent post-Hugo vegetation recovery (Figure 5) was acquired on October 23, 1999. This image was the closest cloud free image to the Hurricane Hugo anniversary date and would display the recovery after a ten-year period. The fourth image (Figure 6) was acquired on October 16, 2011 in order to show the vegetation recovery after a 22-year period. Table 2 provides the characteristics of the images used.

Table 2 Landsat 5 and 7 TM/ETM+ used in the study

Acquisition	Sensor	Spatial Resolution (m)	No. Of Bands
10/30/1987	TM 5	30	7
10/3/1989	TM 5	30	7
10/23/1999	ETM+	30	8
10/16/2011	TM 5	30	7

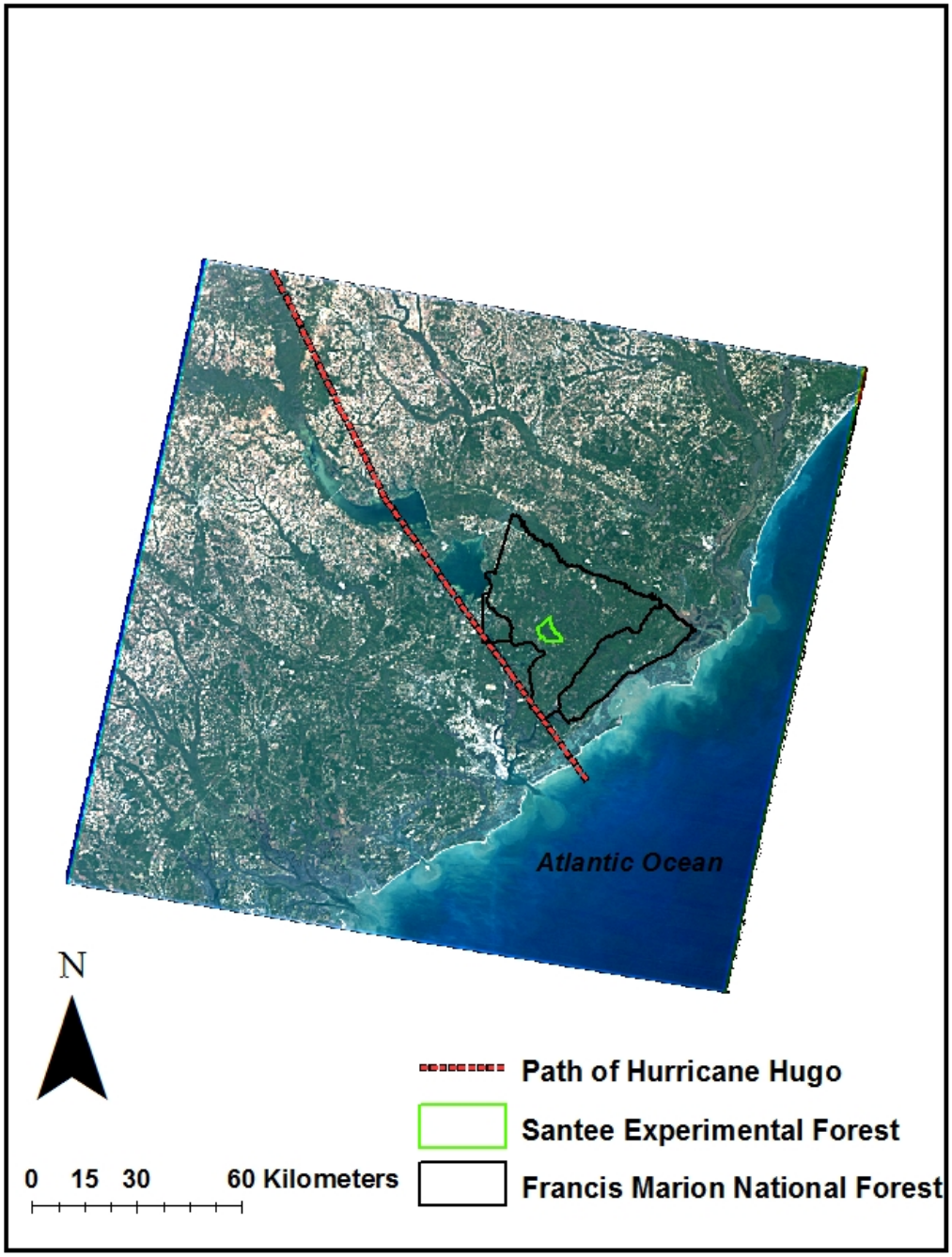

Figure 3 A true color image of Landsat 5 TM image of October 30, 1987 (bands 3,2,1 displayed as red, green, and blue, respectively). The study is outlined in red.

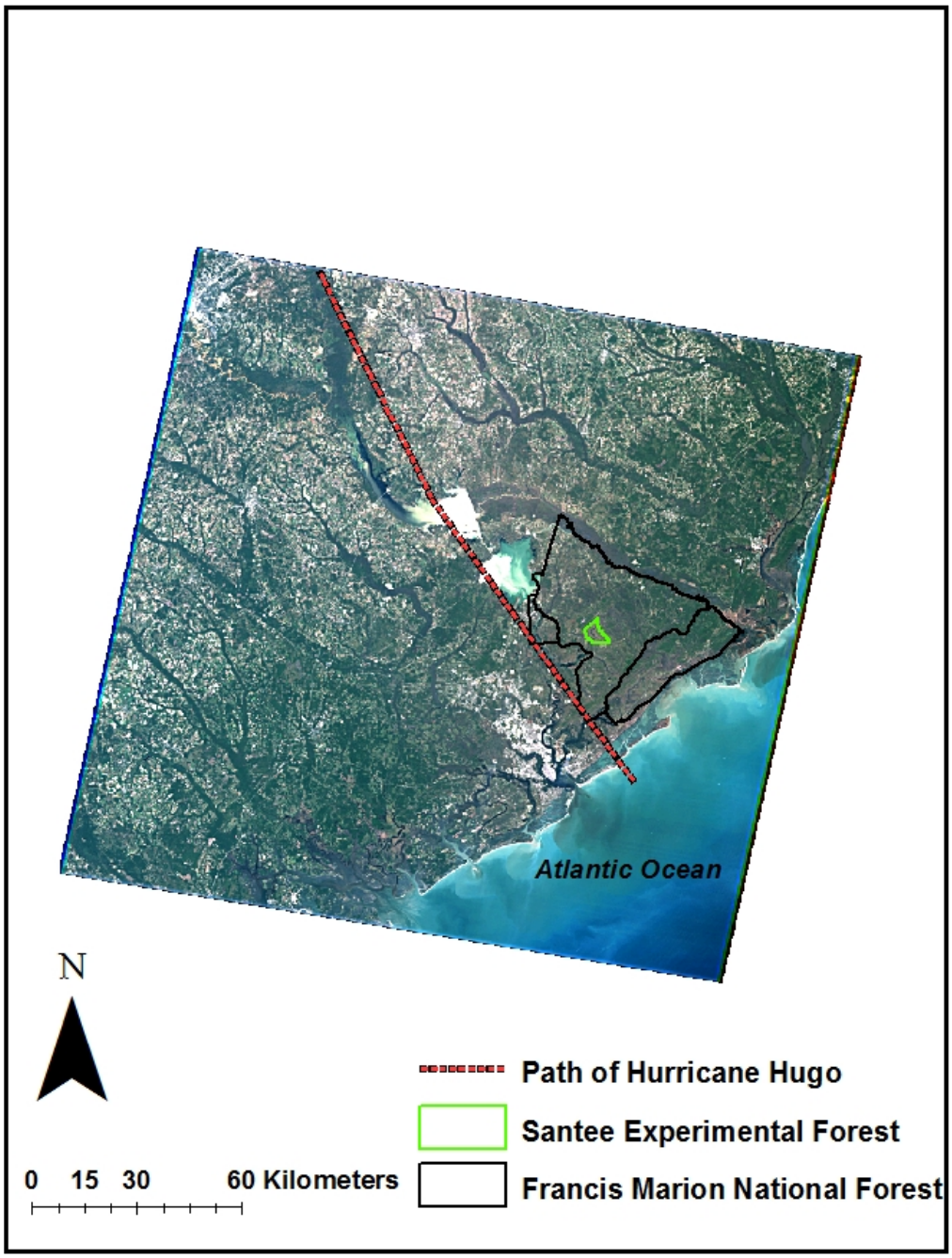

Figure 4 A true color image of Landsat 5 of October 03, 1989 (bands 3,2,1 displayed as red, green, and blue, respectively). The study site is outlined in red.

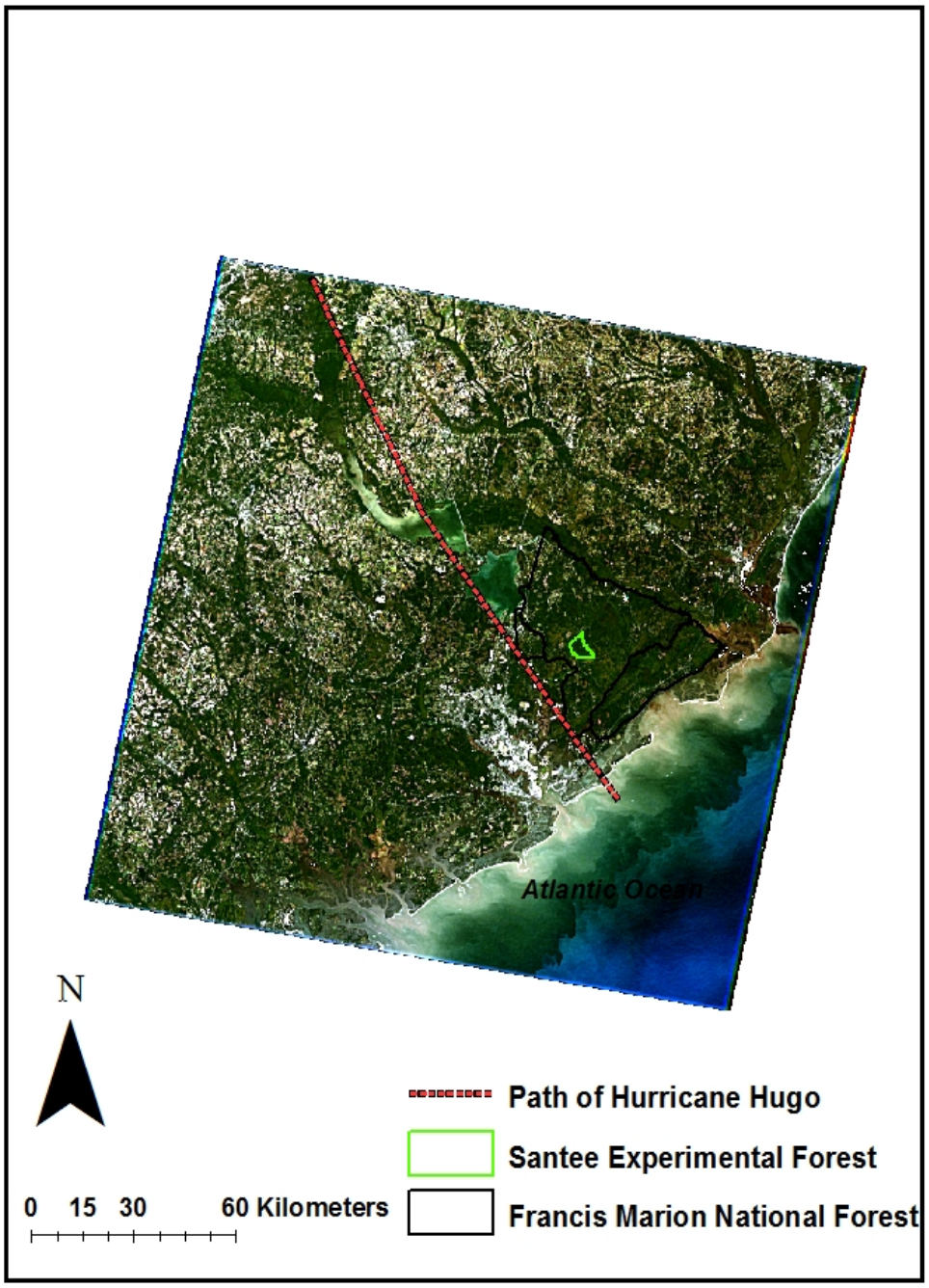

Figure 5 A true color image of Landsat 7 ETM+ October 23, 1999 (bands 3,2,1 displayed as red, green, and blue, respectively). The study is outlined in red.

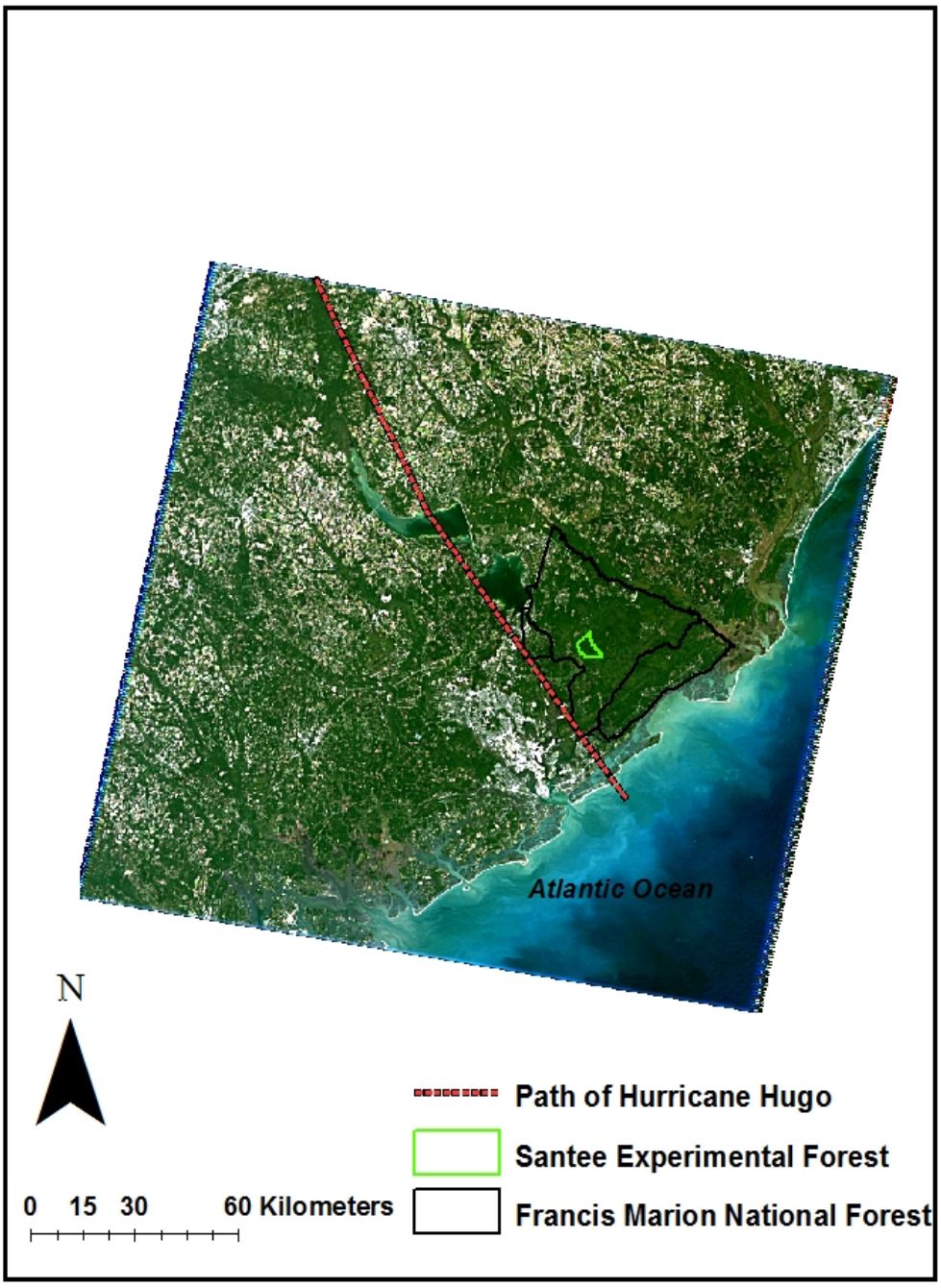

Figure 6 A true color image of Landsat 5 Thematic Mapper of October 16, 2011 (bands 3,2,1, displayed as red, green, and blue, respectively). The study site is outlined in red.

All Landsat scenes were obtained from the United States Geological Survey (USGS) in the form of raw Landsat TM bands. The scene location was based on Land-

sat's Worldwide Reference System (WRS) path 16 and row 37. The images represent the clearest images in the USGS Landsat TM/ETM+ archive for the month of October. The images chosen were cloud free and were taken near the same time each year in order to minimize phenological differences. A subset consisting of the FMNF, located to the North of Charleston, SC where Hurricane Hugo first encountered the South Carolina coast, was selected as shown in Figures 7. The image was then subset an additional time in order to focus on the Santee Experimental Forest (Figure 8).

2.3 Image Processing

Images obtained from the Landsat 5 sensor contain certain levels of noise from atmospheric interference, caused by dispersion of electromagnetic energy, and noise produced from the sensor itself (Kiage et. al., 2007). Atmospheric noise was removed from the images by using ATCOR 2 workstation in ERDAS Imagine 2011, which reduced error. After each image was atmospherically corrected, a subset was then created in order to emphasize the study area (Santee Experimental Forest).

2.4 Data Transformation Methods

Transformation processes help expose changes in surface reflectance that can be used to visualize change in map form. A variety of techniques were utilized in this study, including image classification and NDVI. For image classification, each image was classified into land cover types using spectral reflectance as a point of reference using the unsupervised classification method (Rogers et. al., 2009). This was done using the Interactive Self –Organizing Data Analysis (ISODATA) algorithm from ERDAS 2011 Imagine. This process involves assigning each pixel value within the image a certain land cover classification based on the image's pixel spectral response. Each pixel with similar spectral statistics was aggregated into the same class. Each aggregated spectral clusters was specified as one of the seven major land use/land cover catego-

ries based on the Anderson Classification Scheme (Anderson et. al., 1976) (i.e., 1.water, 2.forested land, 3. marshland, 4. farming (agriculture), 5.barren/damaged forest, 6.urban and build up land, 7.grassland) in order to simplify the analysis of the altered landscape. There are areas within the FMNF with agriculture (Figure 9) and barren (Figure 10) land covers, however these land cover classes were not represented in the SEF. Due to the absence of certain classes (i.e. Water, wetland, and agriculture) within the SEF, only the following classes were used: forest, bare ground, urban, grassland/shrubland, damaged forest and flooded vegetation. Table 3 provides a summary of the land cover classes used in this study.

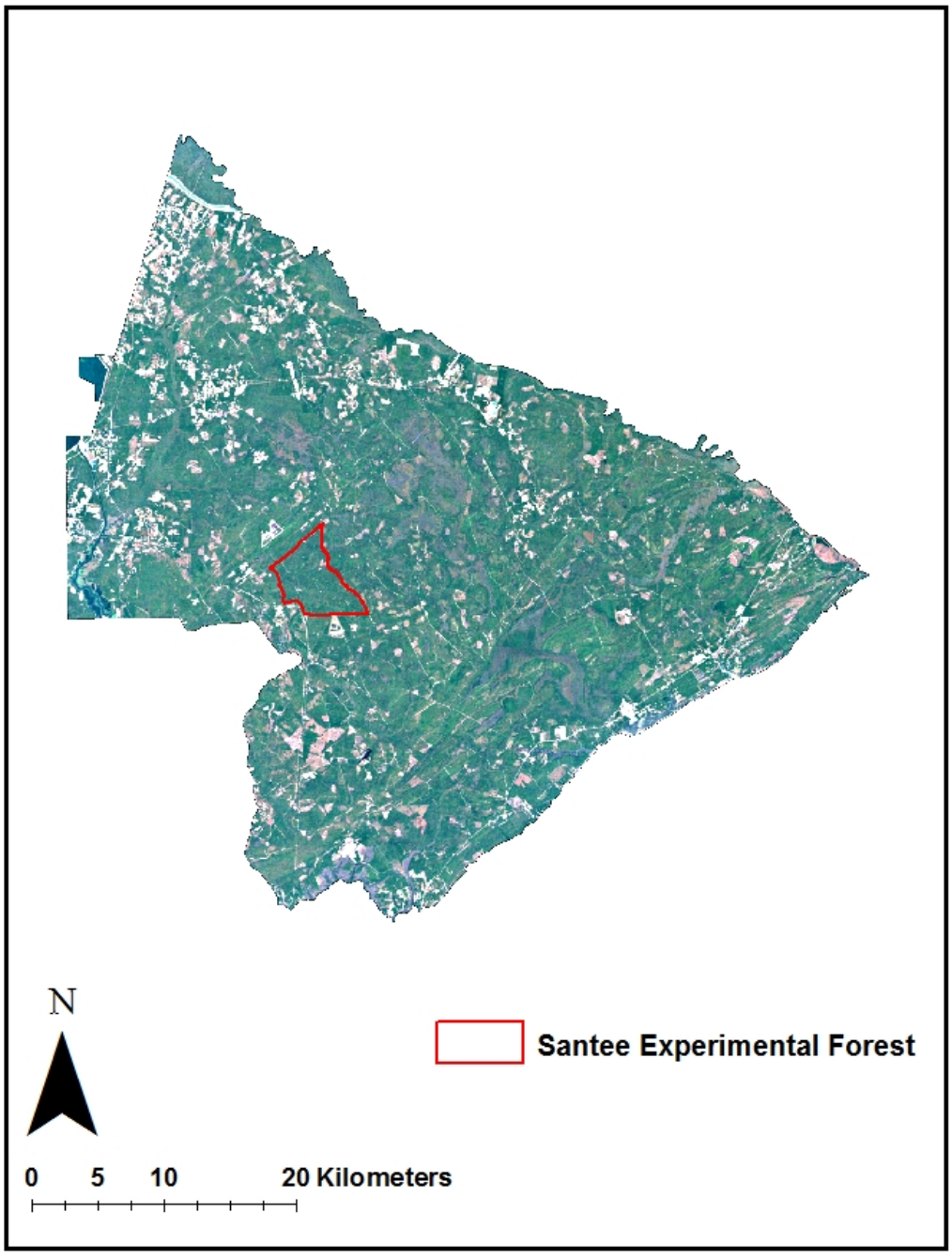

Figure 7 Subset of Francis Marion National Forest on October 30, 1987 (bands 3,2,1 displayed as red, green, and blue, respectively). The study site is outlined in red.

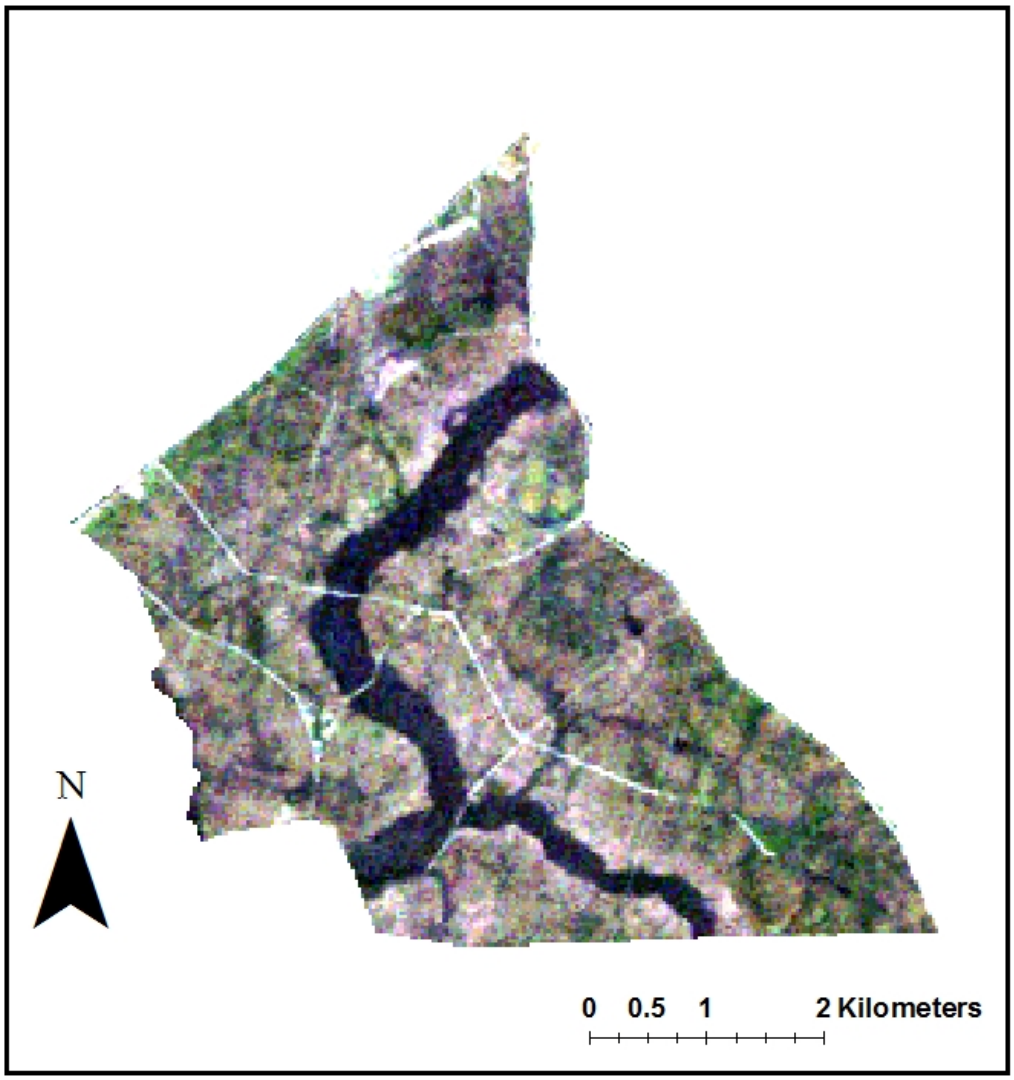

Figure 8 True color Landsat 5 image of Santee Experimental Forest on October 03, 1989 (bands 3,2,1 displayed as red, green, and blue, respectively).

The assignment of each spectral cluster was aided based off visual findings contained in the original images, familiarity with the study area, and matching the latitude and longitude coordinates from the original image with corresponding coordinates on Google Earth.

Figure 9 Agriculture land cover within the FMNF boundary (taken by author on October 7, 2011).

Figure 10 Bare ground area within the FMNF boundary (taken by author on October 7, 2011).

Table 3 Land-cover types used in classification of satellite image.

Land Cover	Code	Description
Forest	1	High density of trees that dominate the canopy.
Bare Ground	2	Soil surfaces that contain minimal vegetation
Urban	3	Built up environments with parking lots, roads, and buildings
Grassland/Shrubland	4	Areas with grass land accompanied by sparse bushes; abandoned agricultural areas
Damaged Forest	5	Areas that experienced vegetation destruction
Flooded Vegetation	6	Areas that experienced flooding

In order to differentiate between spectral clusters and to label the classes accurately, the spectral data layer was placed upon the original image. The opacity for the raster layer was then set to zero. Then the opacity of a single spectral cluster class was

changed to one and assigned a bright color, to highlight the area in which the cluster exists. This technique provided an effective method for determining the location of specific spectral clusters. Once each spectral cluster was assigned a land cover/ land use class, they were subjected to a recoding process. Recoding involves combining similar land cover classes into a single representative class. This resulted in seven land cover classes. The recoded image was then subjected to a suite of filters including the 8 x 8 ha clump and 2 x 2 ha eliminate filters to reduce noise in the classification.

2.5 Accuracy Assessment

Each image was then subjected to an individual accuracy assessment once the final land cover classes were established. Due to the use of historical images for the study, ground referencing was not conducted. The original images and the accuracy assessment tool from ERDAS Imagine 2011 were relied on to conduct the assessment. The tool randomly plotted 50 random points on the original image. The land class in which each point is located was then determined using corresponding latitude and longitude coordinates with Google Earth. The classes of each point were then compared to the original classification and a report was created that showed user's accuracy, producer's accuracy, overall accuracy, errors of emission and a Kappa coefficient. A confusion matrix, which is a cross tabulation of land cover class labels given by the user compared to observed reference data points randomly plotted at different locations was also created (Foody, 2002). The final classification accuracy for each image was determined by dividing the sum of all the correctly classified pixels by the number of pixels in the confusion matrix (Kiage et. al., 2007).

2.6 Change Detection

In this study, four thematic images were created using unsupervised classification from four different time periods, which were compared to each other to determine

the change in vegetation cover. The October 30, 1987 image and the October 3, 1989 image were placed into the matrix tool in the ERDAS Imagine 2011 software. Once the two images were run through the matrix, a single image was produced highlighting the land cover classes that changed. Then the October 3, 1989 and October 23, 1999 re-generation images were subjected to the matrix to determine the land cover change. A change detection matrix was also conducted for the October 23, 1999 and October 16, 2011 images to determine vegetation recovery over a 20-year period

NDVI analysis was performed on each of the images in order to highlight vegetation changes. NDVI values range between -1 and 1. Values above 0.6 include areas of dense vegetation and values below 0 indicate no vegetation (Kiage et. al., 2007). Surfaces that have negative NDVI values contain water or ice (Kiage et. al., 2007). NDVI provides a simplistic approach for differentiating between areas with and without vegetation making the index ideal for this study.

3. RESULTS

3.1 Accuracy Assessment of Classification Results

Tables 4, 5, 6, and 7 are confusion matrices that show user's and producer's accuracy as well as the Kappa statistic for the land cover classification accuracy assessment. The overall accuracy for 1987 was 93%, with a Kappa statistic of 0.723. These results imply that there is coherence between the classification class and the actual land cover with very few misclassifications occurring. The overall accuracy for the October 03, 1989 image was 81% with a Kappa statistic of 0.786. Although the overall agreement was not as strong for this image due to the difficulty in differentiating between damaged

forest, flooded vegetation and the bare ground class, the forest class had a high level of accuracy, which is the class we are mainly focus on. The confusion matrix for the October 23, 1999 image was an improvement on the 1989 classification with an overall classification of 86% with a Kappa statistic of 0.672. The Kappa statistic for the 1999 was low due the low accuracy in the bare ground category, which is minimal in the SEF. The most recent image from October 16, 2011 had the highest overall accuracy with 96% and a Kappa Statistic of 0.985. In this classification, the actual land cover and the classification groups were similar due to the relatively short amount of time that passed since its acquisition date, making it easier to identify land cover classes using Google earth. The ISODATA algorithm was extremely accurate in identifying forested areas in each of the images. The classified images for the SEF are shown in Figure 11-14.

Table 4 Error Matrix of the land-cover classification map derived from the October 30, 1987 Landsat 5 TM image.

Classified Data (land-cover type)	Reference Data 1	2	3	4	5	6	Classified Total	Producer's Accuracy	User's Accuracy
1.Forest	80	3	0	0	0	0	83	100.00%	97.26%
2.Barren	0	7	0	0	0	0	7	50.00%	100.00%
3.Urban	0	4	6	0	0	0	10	60.00%	65.00%
4.Grass/Shrubland	0	0	0	0	0	0	0	0	0
5.Damagede Forest	0	0	0	0	0	0	0	0	0
6.Flooded Vegetation	0	0	0	0	0	0	0	0	0
Reference Total	80	14	6	0	0	0	100		
Overall Classification Accuracy	93%								
Overall Kappa statistics	0.723								

Table 5 Error Matrix of the land-cover classification map derived from the October 03, 1989 Landsat 5 TM image.

Classified Data (land-cover type)	Reference Data 1	2	3	4	5	6	Classified Total	Producer's Accuracy	User's Accuracy

1.Forest	53	3	6	0	0	3	65	84.20%	92.56%
2.Barren	0	4	0	0	0	0	4	94.2%	100.00%
3.Urban	0	3	3	0	0	0	6	50.00%	100.00%
4.Grass/Shrubland	0	0	0	0	0	0	0	0	0
5.Damagede Forest	0	0	0	0	13	2	15	100.00%	60.00%
6.Flooded Vegetation	0	0	0	0	2	8	10	72.8%	83.6%
Reference Total	53	10	9	0	15	13	100		
Overall Classification Accuracy	81%								
Overall Kappa statistics	0.786								

Table 6 Error Matrix of the land-cover classification map derived from the October 23, 1999 Landsat 7 ETM image.

Classified Data (land-cover type)	Reference Data						Classified Total	Producer's Accuracy	User's Accuracy
	1	2	3	4	5	6			
1.Forest	78	0	0	8	0	0	86	92.30%	97.46%
2.Barren	0	5	0	2	1	0	8	94.2%	53.80%
3.Urban	0	0	0	0	0	0	0	0	0
4.Grass/Shrubland	3	0	0	3	0	0	6	50.00%	100.00
5.Damagede Forest	0	0	0	0	0	0	0	0	0
6.Flooded Vegetation	0	0	0	0	0	0	0	0	0
Reference Total	81	5	0	13	1	0	100		
Overall Classification Accuracy	86%								
Overall Kappa statistics	0.672								

Table 7 Error Matrix of the land-cover classification mapr derived from the October 16, 2011 Landsat 5 TM image.

Classified Data (land-cover type)	Reference Data						Classified Total	Producer's Accuracy	User's Accuracy
	1	2	3	4	5	6			
1.Forest	92	0	0	0	0	0	92	100.00%	100.00 %
2.Barren	0	2	0	0	0	0	2	100.00%	100.00 %
3.Urban	0	2	4	0	0	0	6	100.00%	68.52 %

4.Grass/Shrubland	0	0	0	0	0	0	0	0	0
5.Damagede Forest	0	0	0	0	0	0	0	0	0
6.Flooded Vegetation	0	0	0	0	0	0	0	0	0
Reference Total	92	4	4	0	0	0	100		
Overall Classification Accuracy	96%								
Overall Kappa statistics	0.985								

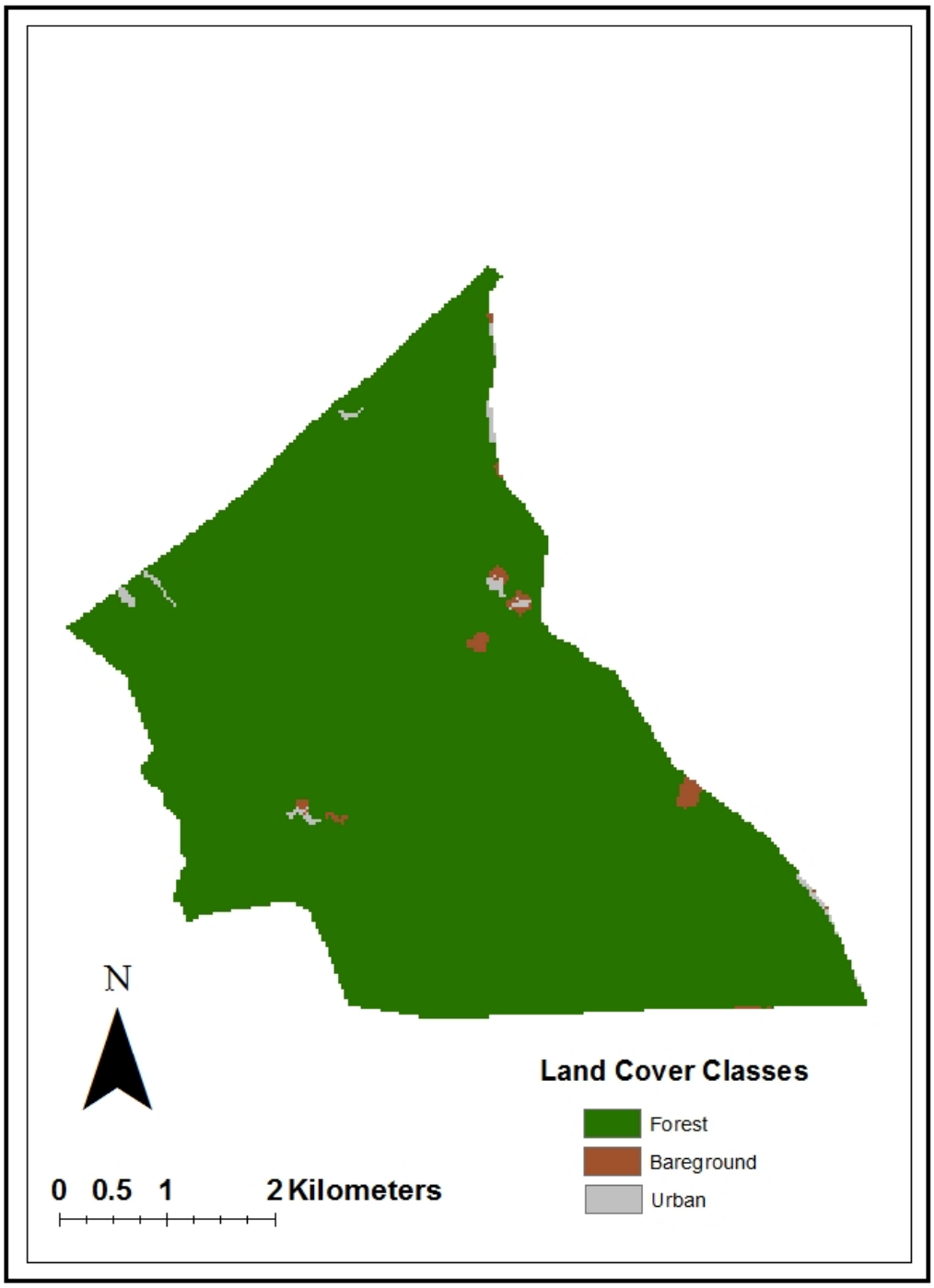

Figure 11 Land-cover map of the Santee Experimental Forest Generated from unsupervised classification of the 1987 TM image.

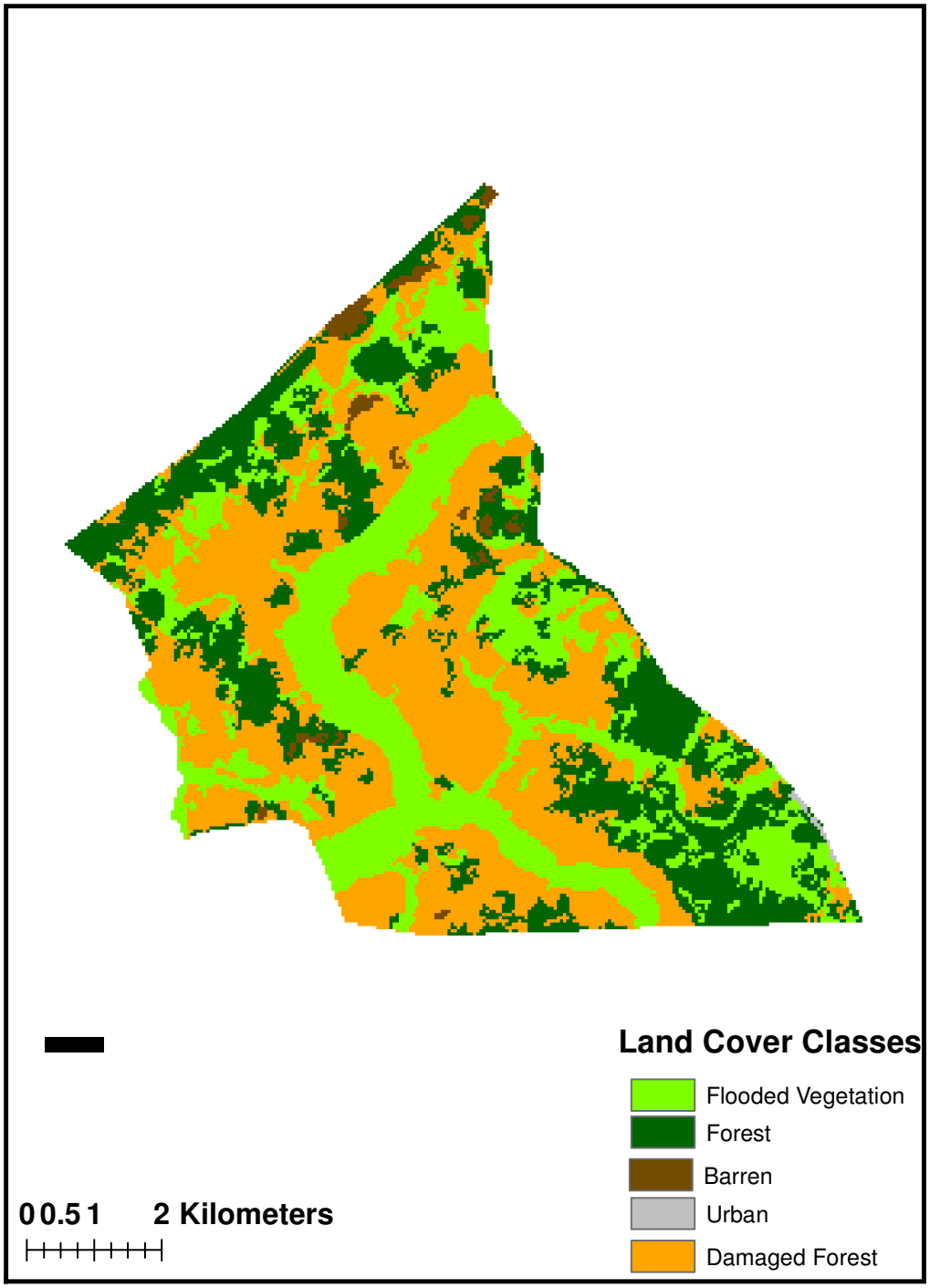

Figure 12 Land-cover map of the Santee Experimental Forest generated from unsupervised classification of the 1989 TM image.

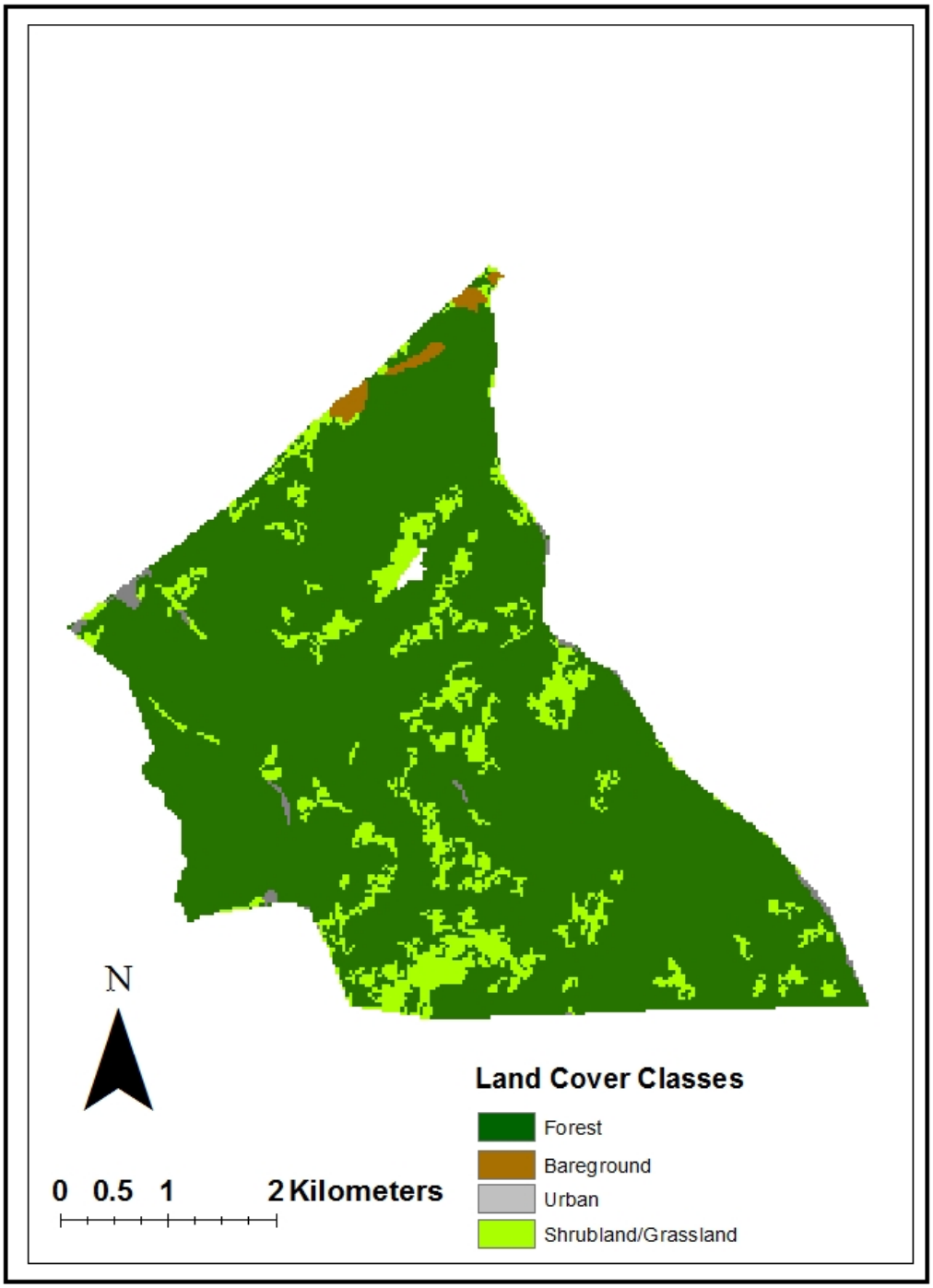

Figure 13 Land-cover map for the Santee Experimental Forest generated from unsupervised classification of the 1999 ETM image.

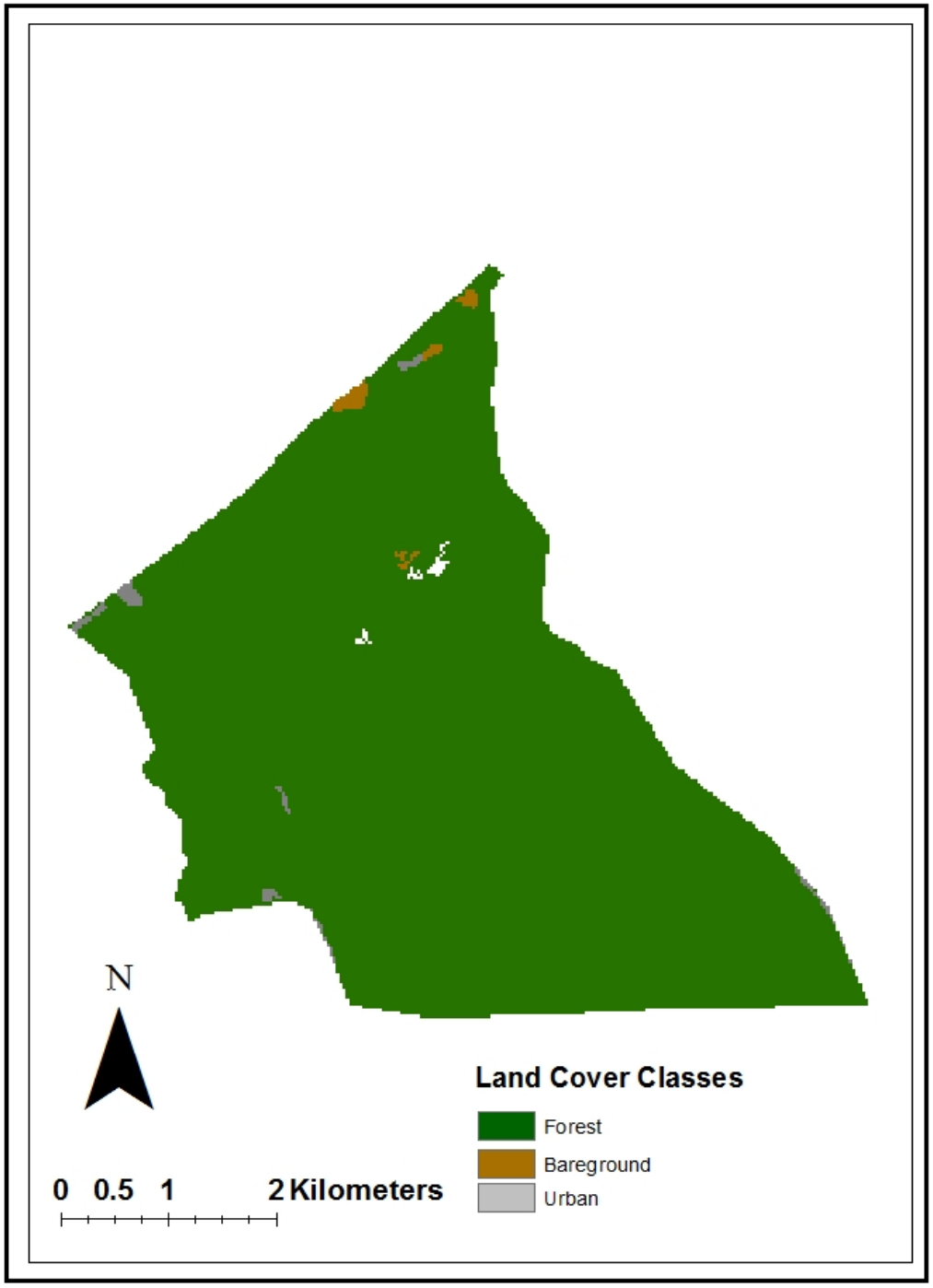

Figure 14 Land-cover map of the Santee Experimental Forest generated from un-supervised classification of the 2011 TM image.

Table 8 Change in land cover from 1987-2011 based off of unsupervised classification.

Classified Data (land-cover type)	1987 (acres)	1989 (acres)	1999 (acres)	2011 (acres)
Forest	6,048	1,587	5,381	6,089
Bare ground	78	90	46	27
Urban	33	7	44	34
Damaged Forest	0	2,624	0	0
Shrubland/Grassland	0	0	679	0
Flooded Vegetation	0	1,851	0	0

3.2 Land Cover Change Detection

The most dominant land cover class in the 1987 classification (pre-Hugo) within the SEF was forest at 6,048 acres (98%) shown in Figure 15. The results for the change detection between October 30, 1987 and October 03, 1989 show the largest land cover change with a 2,624 acre change from forested area to damaged forest and 1,851 from forest to flooded vegetation. Out of the 6,100 acres within the SEF only 1,529 acres remained as forestland cover.

After a 10 year period (1989-199) there was a 3,918 acre change from the damaged forest and flooded vegetation class to the forest class. This equates to a 64% recovery for a 5,381 acres area of forestland cover in 1999, shown in figure 16. After an additional 12 years of recovery (22 years overall) there was 670 acres land cover change from shrubland/ grassland to forested land resulting in 6,089 acres of forestland overall shown in Figure 17.

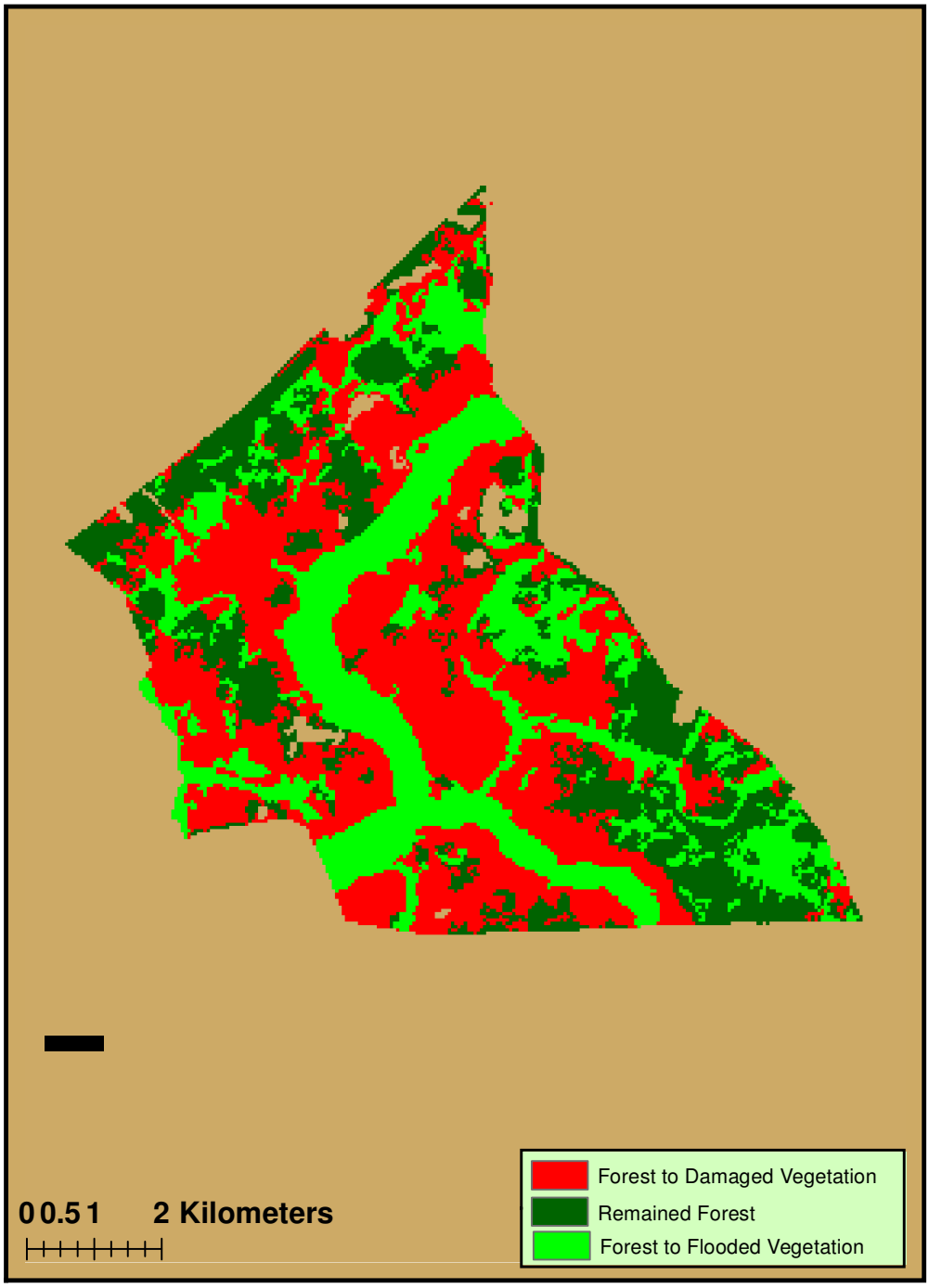

Figure 15 A change-detection map obtained by comparing the 1987 and the 1989 land cover.

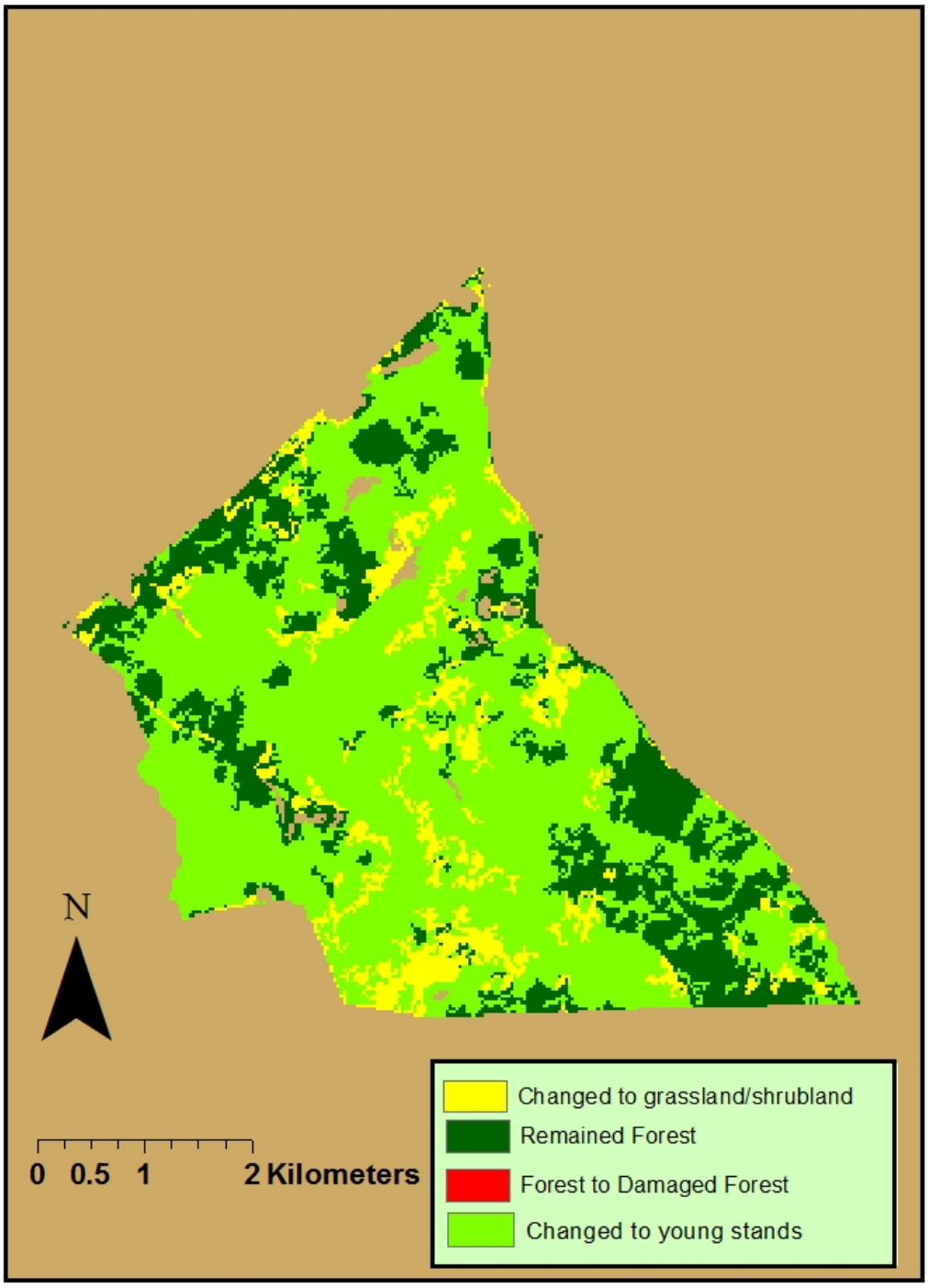

Figure 16 A change-detection map obtained by comparing the 1989 and 1999 land cover.

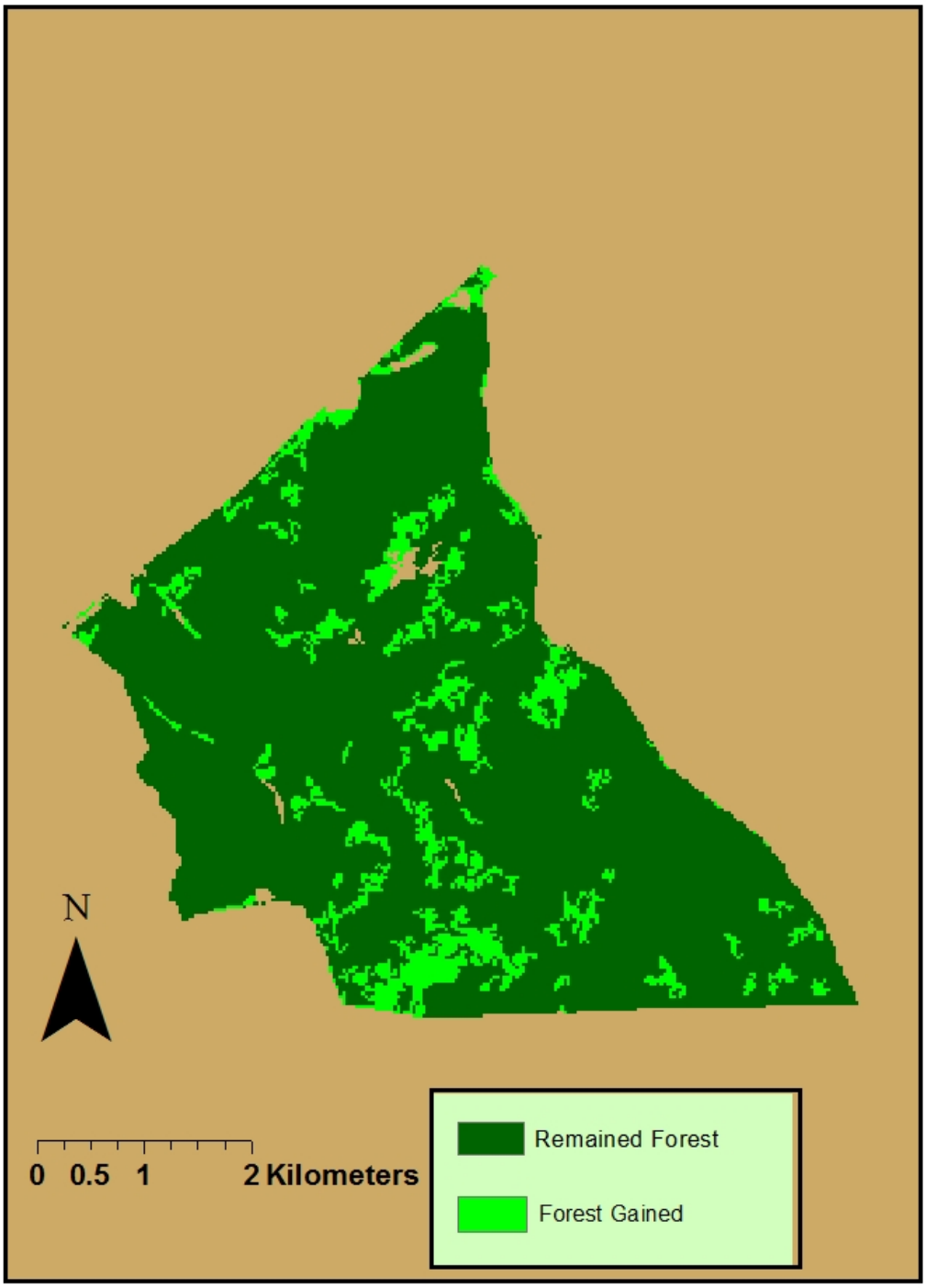

Figure 17 A change-detection map obtained by comparing the 1999 and the 2011 land cover.

3.3 NDVI Result

Table 9 Descriptive statistics for NDVI values.

Images	Mean NDVI	Minimum NDVI	Maximum NDVI	Standard Deviation NDVI
October 30, 1987	0.397	0.027	0.996	0.423
October 03, 1989	0.266	0.062	0.933	0.288
October 23, 1999	0.452	0.128	0.996	0.479
October 16, 2011	0.457	0.023	0.996	0.485

The NDVI images used in this change detection method are shown in Figures 18, 19, and 20. NDVI pixel values vary between -1.0 to +1.0. Values that have a rating less than 0 represent areas that contain high levels of moisture. Areas that display values close to 0 are areas that contain no vegetation (bare ground). Increasing values are indicative of an increase in vegetation cover (Kulkarini, 2004).

The 1987 image (pre-Hugo) had an average NDVI value of 0.397 with the minimum value of 0.027 and a maximum value of 0.996 with a standard deviation of 0.423. The image shows that the majority of the study area is covered with dense vegetation. This result is similar to results from the classification image.

The 1989 image (post-Hugo) had an average NDVI value of 0.266 with the minimum value of 0.0622 and a maximum value of 0.9338 with a standard deviation of 0.288. This image highlights the change from forested area to wetland/flooded vegetation and

damaged vegetation. In general the large decrease in forested area can be seen in the NDVI image (figure 18).

According to the image differencing tool from ERDAS Imagine 2011, 5,986 acres within the SEF experienced a NDVI decrease resulting in an average NDVI value of 0.266 with the, which was the lowest value in the study. After a ten-year (October 03, 1989-October 23, 1999) period 6,162 acres experienced an increase in NDVI resulting in the second highest average NDVI value of 0.452. In 2011, 22 years after Hurricane Hugo showed the highest average NDVI value of 0.457. Table 8 shows the range of NDVI for each of the time periods.

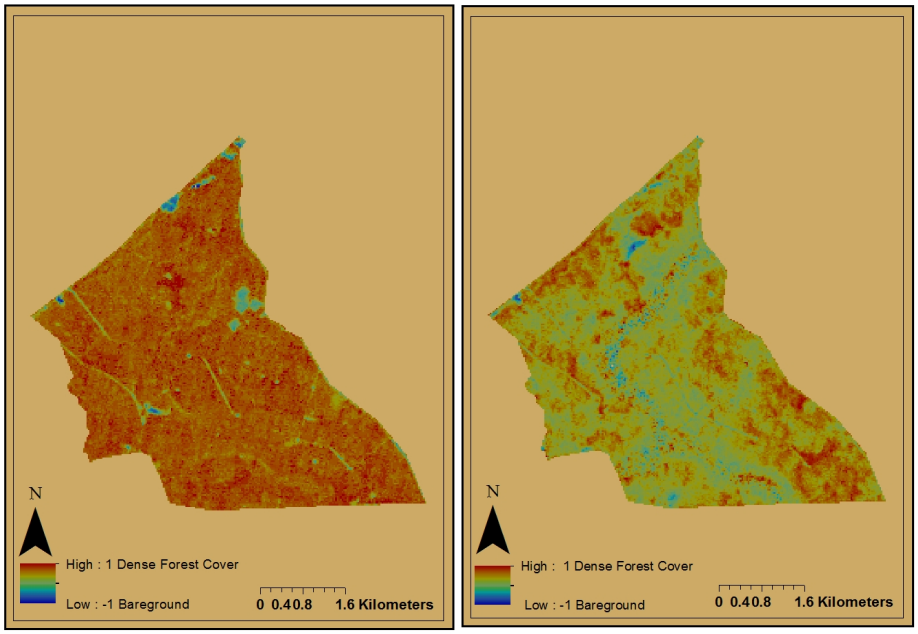

Figure 18 A map of classification based on NDVI values for 1987 and 1989 showing a decrease in forest cover.

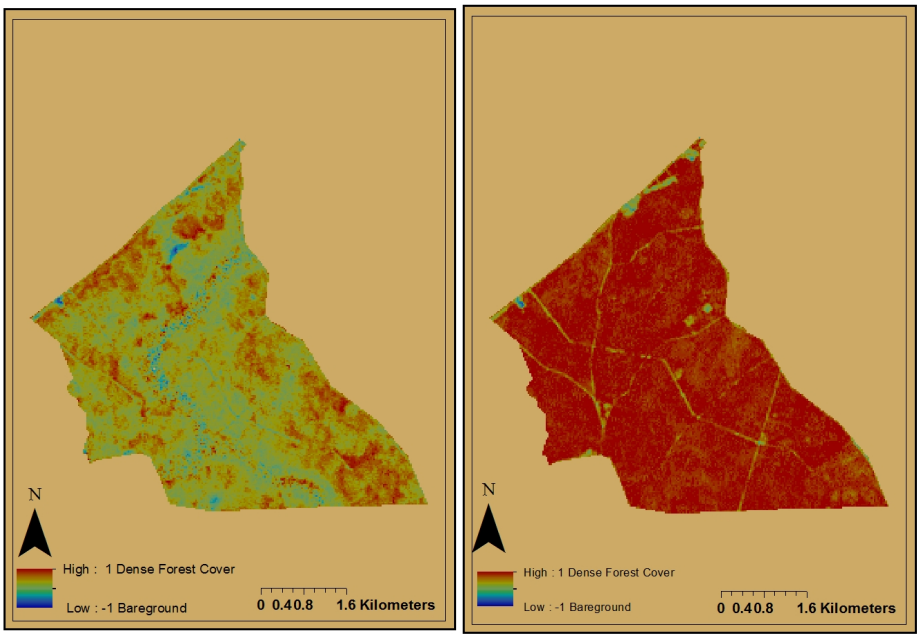

Figure 19 A map of classification based on NDVI values for 1989 and 1999 showing an increase in forest cover.

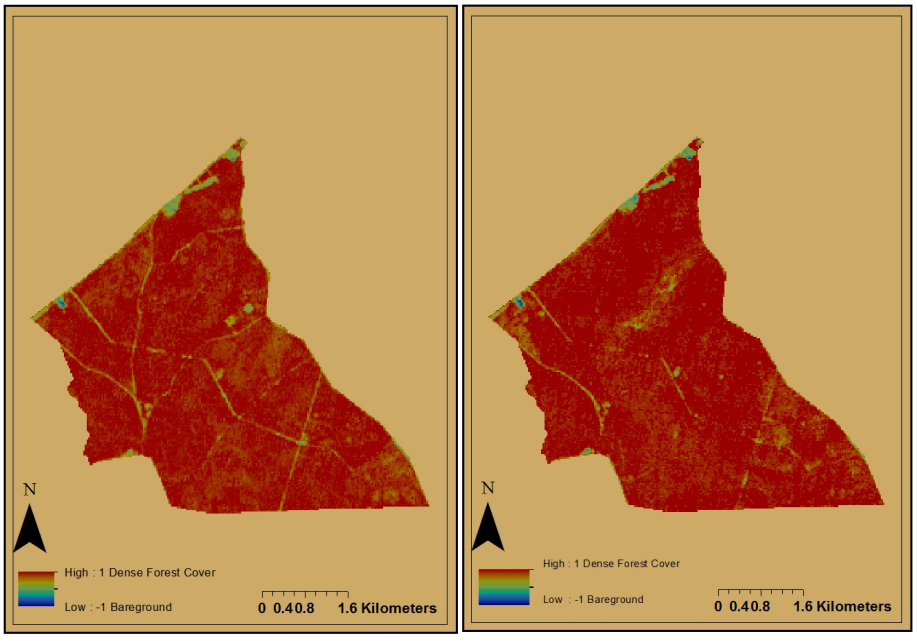

Figure 20 A map of classification based on NDVI values for 1999 and 2001 showing slight increases in forest cover.

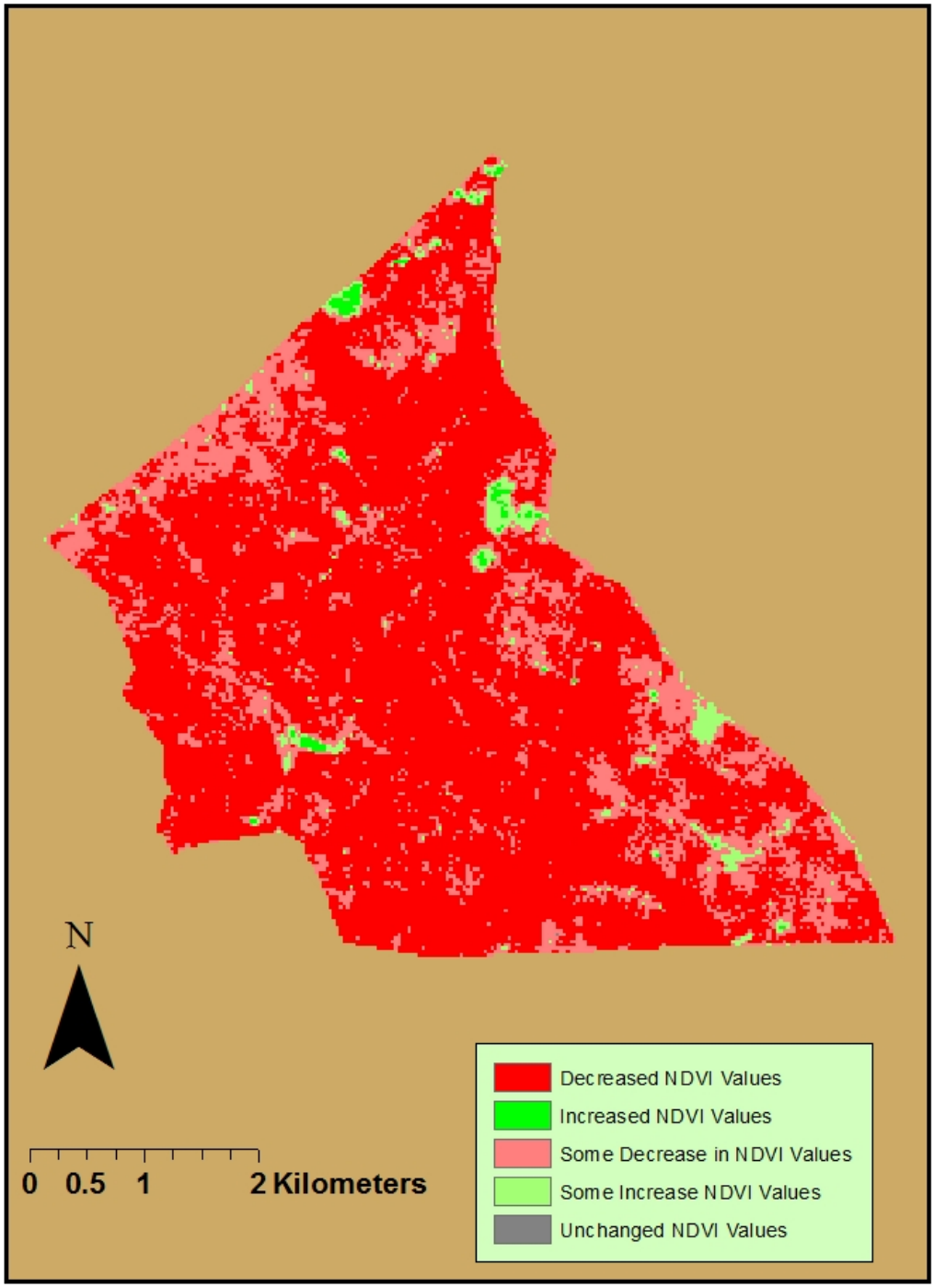

Figure 21 Highlights areas that had altered NDVI values from 1987-1989

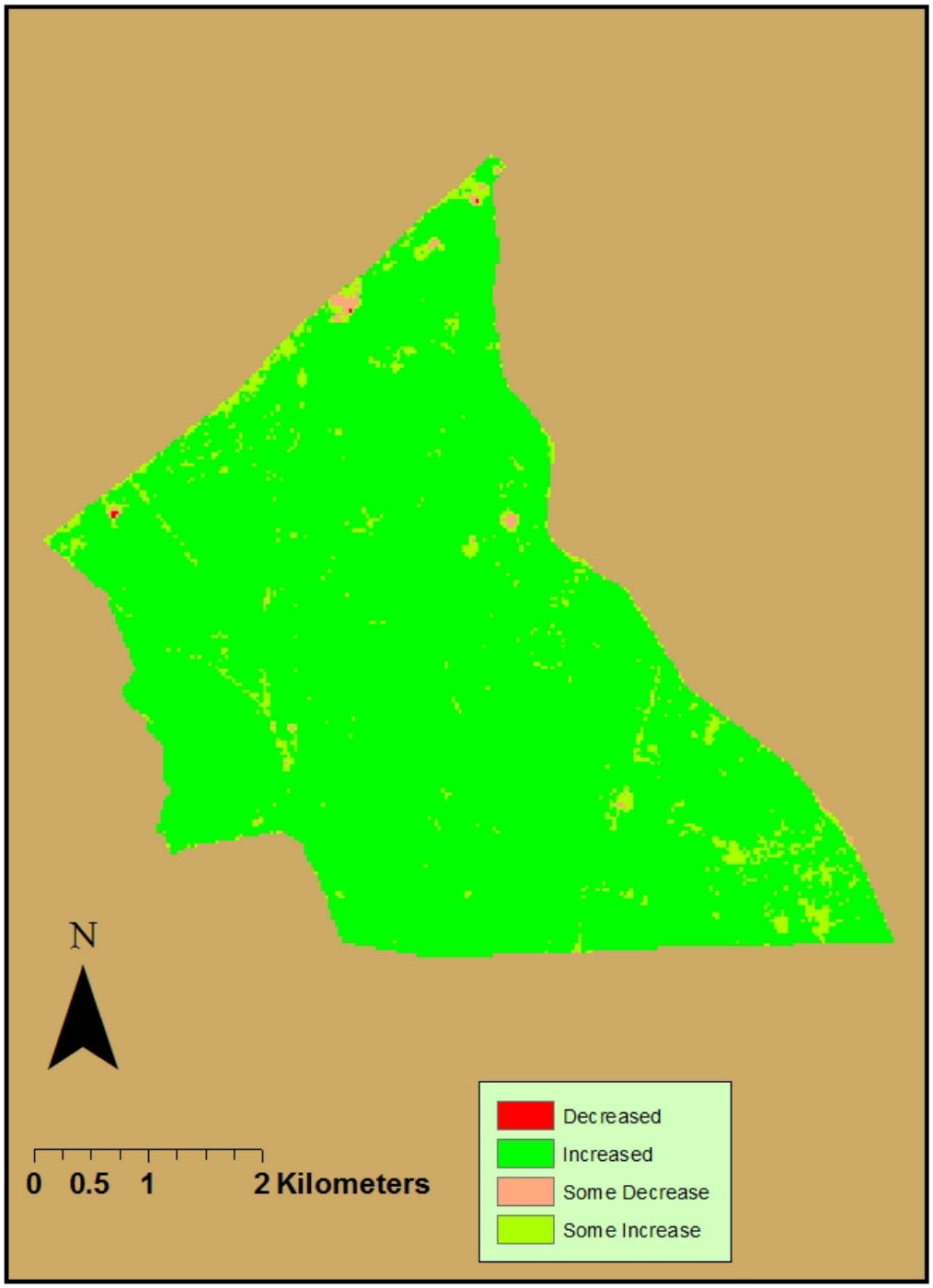

Figure 22 Highlights areas that had altered NDVI values from 1989-1999

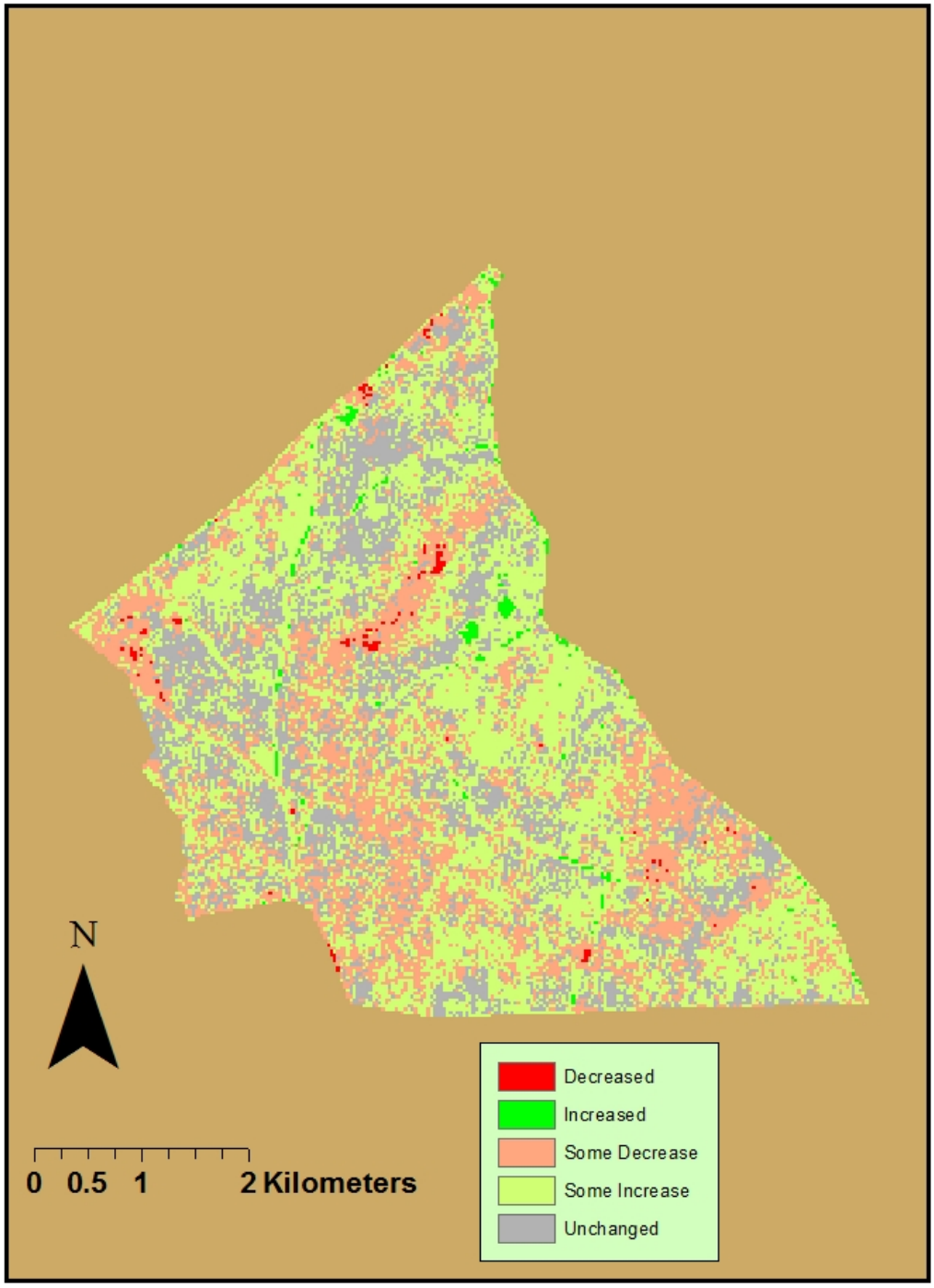

Figure 23 Highlights areas that had slightly altered NDVI values from 1999-2011

Finally, in order to determine if a variation in soil moisture affected NDVI values for the study area, precipitation levels were examined for a period of three months

(July, August, and September) leading up to the image acquisition month of October (Table 9).

Table 10 Precipitation levels for July, August, & September for Charleston, SC. (Source: NOAA 1987, 1989, 1999, & 2011)

Year	July (in)	August (in)	September (in)	Total (in)
1987	2.71	7.85	14.49	25.05
1989	6.15	10.17	13.35	29.67
1999	3.06	2.53	10.81	16.4
2011	5.41	2.63	3.6	11.64

4. DISCUSSION

Hurricanes have the capacity to drastically alter an environment, with both immediate and long-lasting effects. Specifically, when considering mature coastal plain forests, hurricanes can lead to defoliation, snapping, and uprooting of mature tree stands (Cablk et. al., 1994). This type of vegetation damage can permanently alter land cover types, leading to a change in the surrounding areas. Moreover, understanding how certain tree populations react to a hurricane landfall in an area can reveal their susceptibility to reoccurring storms. In the current study, we investigated the initial and sustained impacts of Hurricane Hugo on a coastal plain forest, the Santee Experimental Forest (SEF), which passed through the coast of South Carolina in 1989. The study suggests that the initial impact by Hurricane Hugo on the SEF resulted in a decrease in vegetation cover in the coastal plain forest, primarily in the trees comprising the canopy cover. This initial decrease in vegetation coverage was regenerated in the ten years following the hurricane and has thus remained consistent. The land cover following Hurricane is currently dominated by young growth tree stands, indicating that the hurricane altered the vegetation mosaic of the SEF shown in Figure 24.

Figure 24 Young tree stands within the Santee Experimental Forest (taken by author October 7, 2011).

An overall decrease in initial vegetation coverage within the SEF post-Hugo was measured. The first satellite image measuring vegetation cover was obtained from 1987, two years prior to the hurricane and again 14 days post-hurricane. Vegetation indices measured from Landsat 5 satellite imagery showed a 0.131 reduction in Normalized Differencing Vegetation Index (NDVI) value from October 30, 1987 to October 03, 1989 (date of storm). There are multiple indicators that point to Hurricane Hugo as the reason for this initial mass reduction in vegetation cover. First, Hurricane Hugo was the only significant tropical cyclone within this time period to influence the region. Second, past studies (Cooper-Ellis et. al., 1999 ; Smith, 1997) indicate that high wind speeds are among the most significant factors that cause vegetation damage during a hurricane.

Wind speeds at the study area during Hurricane Hugo were estimated to be 121 miles per hour (Hook et. al., 1991), which explains why up to 74% of the forest was damaged. Thus, it is likely that the reduction in NDVI values is related to the loss of canopy and defoliation caused by the powerful winds from Hurricane Hugo.

Beyond investigating the amount of damage in the SEF caused by Hurricane Hugo, we also investigated the timescales needed for a coastal plain forest to reach recovery in terms of vegetation cover. Considering its location relative the path of the storm, the study site experienced extensive vegetation damage. Due to high wind speeds, vegetation defoliation is the most common effect of hurricanes on forests (Lugo, 2008), while some individuals may also experience snapping and breakage, which would explain the decrease in overall NDVI values for the 1989 post-Hugo image. Foliage height profiles show a clear distinction between canopy defoliation, which exhibits higher levels of defoliation compared with understory defoliation in areas that were affected by hurricane winds (Lugo, 2008). This was consistent in the SEF, the tallest trees sustained the greatest damage from Hurricane Hugo, while the vegetation comprising the understory, suffered less damage (Hook et. al., 1991). In the aftermath of Hurricane Hugo, the canopy was fragmented due to fallen trees and defoliation, which lead to a decrease in chlorophyll activity. Decreased chlorophyll activity may lead to lower absorption rates of the red band, thus resulting in lower NDVI values, which was the expected result.

After the initial decrease in chlorophyll levels, the NDVI values showed that the SEF had a large vegetation cover recovery after a ten-year period (1989-1999). It was not expected that the NDVI values for the 1999 (recovery image) image would surpass the values of the 1987 image (pre-Hugo), only 10 years after Hurricane Hugo. Factors that influence NDVI values were examined to determine the cause of the unexpected

increase. NDVI values are associated with vegetative factors that include growing vegetation, cover percentage, leaf area index, and green biomass (Di et. al., 1994). A large influence in these identifying factors is soil moisture, which is linked to precipitation. In order to determine if a variation in soil moisture affected NDVI values for the study area, precipitation levels were examined for a period of three months (July, August, and September) leading up to the image acquisition month of October (Table 9). Although NDVI levels are influenced by precipitation, in this study, it can be deduced that precipitation levels were not the cause of differentiating NDVI values because 1987 (25.05 in) experienced more precipitation during this time period and still sustained lower NDVI values than in 1999 (16.4 in) and 2011 (11.64 in).

The high NDVI values represented in the two recovery images (1999 and 2011) can be attributed to a drastic change to the forest's environment due to the loss of its canopy. The changes include an increase understory light, temperature increase, and a decrease in relative humidity (Lugo, 2008). Tree fall gaps created by downed trees and defoliation increases the available light, which lead to forest regeneration (Bellingham et. al., 1996). Following Hurricane Hugo the trees comprising the understory received substantially more energy after they were released to the canopy.

The recovery process after a major disturbance such as a hurricane is largely determined by residuals (Chazdon, 2003). Residuals are the organisms or their seeds that survived the disturbance (Turner & Dale, 1998). The recovery process that follows an intense wind event follows a course of secondary succession due to the presence of residuals (Whitemore & Burelsome, 1998). Although, trees may sustain high levels of damage, many species have the ability to resprout (Chazdon, 2003). The understory of the SEF received less damage than the canopy, this combined with increase light expo-

sure allowed residuals from the understory to regenerate, and this would explain the rapid regeneration of vegetation cover.

Older trees exhibit low vitality and contain dead vegetation in the canopy. The presence of canopy gaps would allow opportunity for younger trees to populate. NDVI values for the 1987 pre-Hugo images were lower than the 1999 image due to the presence of younger vegetation in the latter image. The NDVI values for the 1999 images are higher because younger stands are more responsive to phenology in greenness (Song & Woodcock, 2003). The higher NDVI values can be attributed to the growth of new foliation in the canopy (Song & Woodcock, 2003). Furthermore, younger stands have higher NDVI values because the new understory growth has a larger influence on the remotely sensed signal than in old growth stands (Song & Woodcock, 2003). The small increase in NDVI values from 1999 to 2011 can be attributed to the continued growth of younger tree stands.

The results of land cover change detection showed that the largest land cover change between 1987 and 1989 was from forested land to damaged forest/flooded vegetation (4,465) acres. The increase in flooded vegetation can be attributed to the increase in moisture content, which was evident in the post-Hugo classification. The increase in damaged forest is a direct result of the wind trauma experienced by the vegetation during the disturbance. Wind caused defoliation, snapping, and uprooting, which was clearly identified in the unsupervised classification process for the post-Hugo image (1989). Not surprisingly, ten years after Hugo (1999), all flooded vegetation land cover returned to forest cover. This is due to a subsidence of floodwaters within the study area. Areas that were previously damaged vegetation changed to forest cover or grassland/shrubland. Areas that returned to forest cover can be attributed to the regeneration of residuals and pioneering species. After a period of 20 years (2011) the

forest cover in SEF was back to 98% similar to the 1987 image. The results from the land cover change detection are consistent with NDVI values in that much of the vegetation cover returned to the SEF after a 10-year period.

5. SUMMARY OF MAJOR FINDINGS AND RECCOMNEDATIONS FOR FUTURE STUDIES

The objectives for this study were all accomplished, as the study was able to determine the extent of the damage in the Santee Experimental Forest following Hurricane Hugo, monitor the vegetation cover recovery process of the Santee Experimental Forest after a twenty-two year period, and confirm that remote sensing can be used to monitor long-term recoveries in coastal plain forest landscapes. The initial impacts from Hurricane Hugo from 1987-1989 on the SEF vegetation were accurately identified. The forested areas in the SEF were drastically reduced from 6,048 acres to 1,587 acres, which is equivalent to a 74% decrease. Intense winds and flooding from Hugo contributed to 4,465 acres of damaged forest and flooded vegetation. The 1987-1989 changes were clearly depicted in the unsupervised classification and were supported by the NDVI values due to the decrease in chlorophyll activity.

The 1999 unsupervised classification image showed a 64% forest cover regeneration from 1989 and an additional 11% by 2011. Although the forest cover was more extensive in the 1987 image compared to the 1999 image, the NDVI values were higher for the latter. The NDVI values for the 2011 images exhibited an increase as well, but at a slower rate. This can be explained by the increase in young vegetation. The phenology in younger tree stands are more responsive to the NDVI band combination because growing vegetation has a lower red reflectance due to the absorption by chlorophyll, whereas stands that contain an aging canopy contain dead vegetation that is no longer

active. This proved the final objective of the study, which was to confirm that NDVI can be used to monitor forest recovery.

The recovery in vegetation cover after a 22-year period provided an example of the resilience of a coastal plain forest after a large disturbance. Throughout the course of the study, new questions evolved that require additional investigation. Future studies are needed to determine the recovery timescales needed by other forest types that are subjected to frequent hurricane activity. Furthermore, future research can continue to monitor the SEF recovery to determine when NDVI values return to pre-Hugo level, this will show the full recovery process.

6. CONCLUSION

This study shows that Landsat TM images combined with remote sensing techniques such as NDVI and the ISODATA algorithm can be utilized to help monitor the initial effects and recovery of vegetation cover in a coastal plain forest. These techniques can be used by the forest service to determine stands that are recovering successfully from a large natural disturbance over long periods of time, with relative low cost compared to field surveys.

REFERENCES

Aldrich, R. (1975). Detecting disturbances in a forest environment. *Photogrammetric Engineering and Remote Sensing, 41*, 39-48.

Anderson, J., Hardy, E., Roach, J., Witmer, R.,. (1976). *A Land Use And Land Cover Classification System For Use With Remote Sensor Data*.

Anderson, J., & Perry, J. (1996). Characterization of wetland plant stress using leaf spectral reflectance: Implications for wetland remote sensing. *Wetlands, 16*(4), 477-487.

Bellingham, P., Tanner, E., Rich, P., & Goodland, T.,. (1996). Changes in Light Below the Canopy of a Jamaican Montane Rainforest After a Hurricane. *Journal of Tropical Ecology, 12*, 699-722.

C. A. Gresham, T. M. W. a. D. J. L. (1991). Hurricane Hugo Wind Damage to Southeastern U.S. Coastal Forest Tree Species. *The Association for Tropical Biology and Conservation, 23*(4), 420-426.

Cablk, M., Michener, W., & Jensen, J.,. (1994). Impacts of Hurricane Hugo on a Coastal Forest: Assesment Using Landsat ™ Data. *Geocarto International 2*, 15-24.

Chazdon, R. (2003). Tropical Forest Recovery: Legacies of Human Impact and Natural Disturbances. *Perspectives in Plant Ecology, Evolution and Systematics, 6*, 51-71.

Colwell J. E., D. G., and Thomason F., . (1998). *Detection and measurement of changes in the production and quality of renewable resources*.

Conner, W. H. (1995). Woody plant regeneration in three South Carolina Taxodium/Nyssa stands following Hurricane Hugo. *Ecological Engineering, 4*(4), 277-287.

Conner, W. H., & Wayne Inabinette, L. (2003). Tree growth in three South Carolina (USA) swamps after Hurricane Hugo: 1991-2001. *Forest Ecology and Management, 182*(1-3), 371-380.

Cooper-Ellis, S., Foster, D., Carlton, G., Lezberg, A.,. (1999). Forest Response to Catastrophic Wind: Results from an Experimental Hurricane. *Ecology, 80*(8), 2683-2696.

Coppin P., J. I., Nackaerts K., Muys B., & Lambin E., . (2004). Digital change detection methods in ecosystem monitoring: a review. *Remote Sensing, 25*, 1565-1596.

Di, L., Rundquist, D., Had, L.,. (1994). Modelling Relationships Between NDVI and Precipitation During Vegetative Growth Cycles. *International Journal of Remote Sensing, 15*(10), 2121-2136.

Dunninf, J., & Watts, B.,. (1991). Habitat occupancy by Bachman's sparrow in the Francis Marion national forest before and after hurricane Hugo. *108*(3).

Feely, K. J., Gillespie, T.W., Terborgh, J.W. (2005). The Utility of Spectral Indices from Landsat ETM+ for Measuring the Structure and Composition of Tropical Dry Forests. . *Remote Sensing 25*, 1565-1596.

Foody, G. M. (2002). Status of land cover classification accuracy assessment. *Remote Sensing of Environment, 80*(1), 185-201.

Foster, D. (1988). Species and Stand Response to Catastrophic Wind in the Central New England, U.S.A. . *Journal of Ecology, 76*, 135-151.

Frangi, J. L., & Lugo, A. E. (1998). A Flood Plain Palm Forest in the Luquillo Mountains of Puerto Rico Five Years After Hurricane Hugo1. *Biotropica, 30*(3), 339-348.

Hook, D. D., Buford M.A., & Williams T.M., . (1991). Impact of Hurricane Hugo on the South Carolina Coastal Plain Forest. *Journal of Coastal Research, 18*, 291-300.

Jensen, J. R., Hodgson, M. E., Christensen, E., Mackey, H. E. J., Tinney, L. R., & Sharitz, R. (1985). *Remote sensing inland wetlands: a multispectral approach* (No. DP-MS-85-68; Other: ON: DE85017060 United StatesOther: ON: DE85017060Wed Feb 06 22:06:45 EST 2008NTIS, PC A03/MF A01; 1.EDB-85-141659English).

Kiage L., L. K., Walker N., Lam N., and Huh, O. (2007). Recent land-cover/use change associated with land degradation in the Lake Baringo catchment, Kenya, East Africa: evidence from Landsat TM and ETM+. *International Journal of Remote Sensing, 28*, 4285-4309.

Kulkarini, A. (2004). Evaluation of the Imapacts of Hurricane Hugo on the Land Cover of Francis Marion Forest, South Carolina Using Remote Sensing. *Master's Thesis*.

LeGrand. (1990). *The Changing Seasons*.

Lugo, A. E. (2008). Visible and Invisible Effects of Hurricanes on the Forest Ecosystems: An International Review. *Austral Ecology, 33*, 368-398.

Myneni, B., Hall, F., Sellers, P., Marshak, A.,. (1995). The Interpretation of Spectral Vegetation Indexes. *Transactions on Geosciences and Remote Sensing, 33*, 481-486.

Ozesmi, S. L., & Bauer, M. E. (2002). Satellite remote sensing of wetlands. [Article]. *Wetlands Ecology & Management, 10*(5), 381-402.

Park A. B., H. R. A., Hicks G. M., Peterson C. J.,. (1983). Multitemporal change detection techniques for the identification and monitoring of forest disturbances. *Proceedings of the 17th International Symposium on Remote Sensing of Environment*, 77-97.

Ramsey, E., Hodgson, M., Sapkota, S., & Nelson, G.,. (2001). Forest Impact Estimated with NOAA AVHRR and Landsat ™ data Related to an Emperical Hurricane Wind-Field Distribution. *Remote Sensing of Environment, 77*, 279-292.

Ramsey E., R. A., Middleton B., Lu, Z. . (2009). Satellite Optical and Radar Data Used to Track Wetland Forest Impact and Short Term Recovery from Hurricane Katrina. *Societies of Wetland Scientists, 29*, 66-79.

Rogers, J., Murrah, A., Cooke, W.,. (2009). The Impact of Hurricane Katrina on the Coastal Vegetation of the Weeks Bay Reserve, Alabama from NDVI Data. *Estuaries and Coasts, 32*, 496-507.

Russell, K. R., Guynn Jr, D. C., & Hanlin, H. G. (2002). Importance of small isolated wetlands for herpetofaunal diversity in managed, young growth forests in the

Coastal Plain of South Carolina. *Forest Ecology and Management, 163*(1,Äì3), 43-59.

Shuman, C. S., & Ambrose, R. F. (2003). A Comparison of Remote Sensing and Ground-Based Methods for Monitoring Wetland Restoration Success. *Restoration Ecology, 11*(3), 325-333.

Smith, G., Nicholas, N., Zedaker, S.,. (1997). Succession Dynamics in a Maritime Forest Following Hurricane Hugo and Fuel Reduction Burns. *Forest Ecology and Management, 95*, 275-283.

Song, C., & Woodcock, C.,. (2003). Monitoring Forest Succession with Multitemporal Landsat Images: Factors of Uncertainty *Transactions on Geoscience and Remote Sensing, 41*(11), 2557-2567.

Supervisor, F. M. (1995). *Summary of Results 6 Year Activity Evaluation*.

Townsend, P. a. W., S. (2001). Remote sensing of forested wetlands: application of multitemporal and multispectral satellite imagery to determine plant community composition and structure in southeastern USA. . *Plant Ecology, 157*, 129-149.

Turner, M., Dale, V.,. (1998). Comparing Large Infrequent Disturbances: What Have We Learned? *Ecosystems, 1*, 493-496.

Wang, W., Qu, J. J., Hao, X., Liu, Y., & Stanturf, J. A. (2010). Post-hurricane forest damage assessment using satellite remote sensing. *Agricultural and Forest Meteorology, 150*(1), 122-132.

Whitemore, T., & Burslem, D,. (1998). Major Disturbances in Tropical Rainforests Dynamics of Tropical Communities *Black* (pp. 549-565). Oxford: Blackwell Science.